Laramide basement deformation in the northern Gallatin Range and southern Bridger Range, southwest Montana
by Erick WB Miller

A thesis submitted in partial fulfillment of the requirements for the degree of Master of Science in Earth Sciences
Montana State University

Abstract:
The mechanical response of Archean "basement" rocks in the cores of Laramide uplifts has received experimental attention, but there have been relatively few field studies documenting Laramide basement behavior. The purpose of this study is to field test existing theoretical basement strain models by documenting the geometry and kinematics of deformation in areas of good exposures. Field studies along well exposed Squaw Creek fault and Canyon Mountain anticline, Gallatin Range, and three anticlines of the southern Bridget Range, southwest Montana, were made by comparing foliations, mesoscopic faults, and slickensides found in basement rocks to Laramide features found in the overlying Cambrian strata.

The results show that in regions where the angle of discordance between the base of the Cambrian and Archean metamorphic foliation surfaces was low (Bridget Range anticlines and Canyon Mountain anticline), the basement deformed by oblique flexural-slip on preexisting foliation surfaces. Passive-slip was important in regions where Archean folds blocked foliation parallel slip. Large (12 meter thick) internally undeformed blocks indicate break up of the folded layer into macrogranular segments was preferred over coherent deformation. Deformation in bounding shear zones occurred under sub-greenschist conditions. Decreased grain size and increased fluid influx accompanied a transition from mechanical fracturing and frictional sliding to pressure solution slip. These observations indicate a fold strain model and are compatible with the fold-thrust model (Berg, 1962).

At Squaw Creek fault in the northwestern Gallatin Range, the angle of discordance between the sedimentary cover and basement foliation was high (80°). The absence of rotated foliation surfaces and a planar upper basement surface indicate a rigid basement response at Squaw Creek. Slickensides indicate left-lateral reverse slip where footwall strain was accommodated by synthetic, foliation-parallel Riedel shears. These observations most closely resemble the thrust-fold model (Erslev, 1986; Stone, 1984), although no force-folding of the sedimentary cover was observed.

Integration of this study with other field studies on Laramide basement deformation indicates that folding of the basement occurred by a spectrum of mechanisms ranging from passive-slip to flexural-slip folding to cataclastic flow. These field observations indicate that compressive buckling of the sedimentary cover was accompanied by active basement folding.

LARAMIDE BASEMENT DEFORMATION IN THE NORTHERN GALLATIN RANGE AND SOUTHERN BRIDGER RANGE, SOUTHWEST MONTANA

by

Erick W. B. Miller

A thesis submitted in partial fulfillment
of the requirements for the degree

of

Master of Science

in

Earth Sciences

MONTANA STATE UNIVERSITY
Bozeman, Montana

June, 1987

APPROVAL

of a thesis submitted by

Erick W. B. Miller

This thesis has been read by each member of the thesis committee and has been found to be satisfactory regarding content, English usage, format, citations, bibliographic style, and consistency, and is ready for submission to the College of Graduate Studies.

June 22, 1987
Date

D R Cooper
Chairperson, Graduate Committee

Approved for the Major Department

June 18, 1987
Date

Stephen G. Custer
Head, Major Department

Approved for the College of Graduate Studies

7.1.87
Date

M B Malone
Graduate Dean

STATEMENT OF PERMISSION TO USE

In presenting this thesis in partial fulfillment of the requirements for a master's degree at Montana State University, I agree that the Library shall make it available to borrowers under rules of the Library. Brief quotations from this thesis are allowable without special permission, provided that accurate acknowledgment of source is made.

Permission for extensive quotation from or reproduction of this thesis may be granted by my major professor, or in his/her absence, by the Director of Libraries when, in the opinion of either, the proposed use of the material is for scholarly purposes. Any copying or use of the material in this thesis for financial gain shall not be allowed without my permission.

Signature Eric V. Miller

Date June 18, 1987

ACKNOWLEDGMENTS

First and foremost, I would like to thank Dr. David R. Lageson for his guidance and insight into the problems of Laramide basement deformation. Suggestions and constructive criticisms from Dr. David W. Mogk and Dr. James G. Schmitt were a great help in the preparation of this thesis. I would like to express my gratitude to Dr. Chris Schmidt for showing me the London Hills anticline and taking a genuine interest in this project. Special thanks are extended to Martina Johnson for her patience and hard work as a field assistant.

Funding provided by Marathon Oil Company and Tenneco Oil Company supported the field work and facilitated the completion of this study. Graduate study at Montana State University was supported by a research assistantship and a scholarship from the Billings Geophysical Society. Finally, I would like to thank my parents, Howard and Ruth Miller. Without their support, this project would not have been possible.

TABLE OF CONTENTS

TABLE OF CONTENTS--Continued

LIST OF TABLES

LIST OF FIGURES

LIST OF FIGURES--Continued

LIST OF FIGURES--Continued

ABSTRACT

The mechanical response of Archean "basement" rocks in the cores of Laramide uplifts has received experimental attention, but there have been relatively few field studies documenting Laramide basement behavior. The purpose of this study is to field test existing theoretical basement strain models by documenting the geometry and kinematics of deformation in areas of good exposures. Field studies along well exposed Squaw Creek fault and Canyon Mountain anticline, Gallatin Range, and three anticlines of the southern Bridger Range, southwest Montana, were made by comparing foliations, mesoscopic faults, and slickensides found in basement rocks to Laramide features found in the overlying Cambrian strata.

The results show that in regions where the angle of discordance between the base of the Cambrian and Archean metamorphic foliation surfaces was low (Bridger Range anticlines and Canyon Mountain anticline), the basement deformed by oblique flexural-slip on preexisting foliation surfaces. Passive-slip was important in regions where Archean folds blocked foliation parallel slip. Large (12 meter thick) internally undeformed blocks indicate break up of the folded layer into macrogranular segments was preferred over coherent deformation. Deformation in bounding shear zones occurred under sub-greenschist conditions. Decreased grain size and increased fluid influx accompanied a transition from mechanical fracturing and frictional sliding to pressure solution slip. These observations indicate a fold strain model and are compatible with the fold-thrust model (Berg, 1962).

At Squaw Creek fault in the northwestern Gallatin Range, the angle of discordance between the sedimentary cover and basement foliation was high (80^{o}). The absence of rotated foliation surfaces and a planar upper basement surface indicate a rigid basement response at Squaw Creek. Slickensides indicate left-lateral reverse slip where footwall strain was accommodated by synthetic, foliation-parallel Riedel shears. These observations most closely resemble the thrust-fold model (Erslev, 1986; Stone, 1984), although no force-folding of the sedimentary cover was observed.

Integration of this study with other field studies on Laramide basement deformation indicates that folding of the basement occurred by a spectrum of mechanisms ranging from passive-slip to flexural-slip folding to cataclastic flow. These field observations indicate that compressive buckling of the sedimentary cover was accompanied by active basement folding.

INTRODUCTION

Study Purpose

Basement-cored uplifts with intervening basins characterize Laramide-style deformation in the northern Rocky Mountain foreland (Figure 1). The question of whether the basement rocks in the cores of Laramide uplifts deformed in a rigid or non-rigid style has been the subject of lively debate for decades (e.g. Berg 1962; Prucha and others, 1965; Stearns, 1978; Blackstone, 1981; Brown, 1983; Matthews, 1986). From experimental investigations and cursory field studies, fold (Berg, 1962) and non-fold (Stearns, 1978) strain models for Laramide basement deformation have emerged.

In the non-fold model, the basement was uplifted in rigid, internally undeformed, fault-bound blocks (Stearns, 1978; Erslev, 1986). The overlying sedimentary cover is force-folded (drape-folded) over the basement during deformation. In the fold model, the basement behaved as a nonrigid body that deformed internally by cataclastic flow (Chappin and Nelson, 1986; Cook, 1983; Hudson, 1955), flexural-slip (Wagner, 1957; Schmidt and Garihan, 1983), or by passive-slip folding (Barnes and Houston, 1970; Spang and others, 1985). Compressive buckling of the overlying sedimentary strata accompanied active basement folding in this model (Berg, 1962; Brown, 1983).

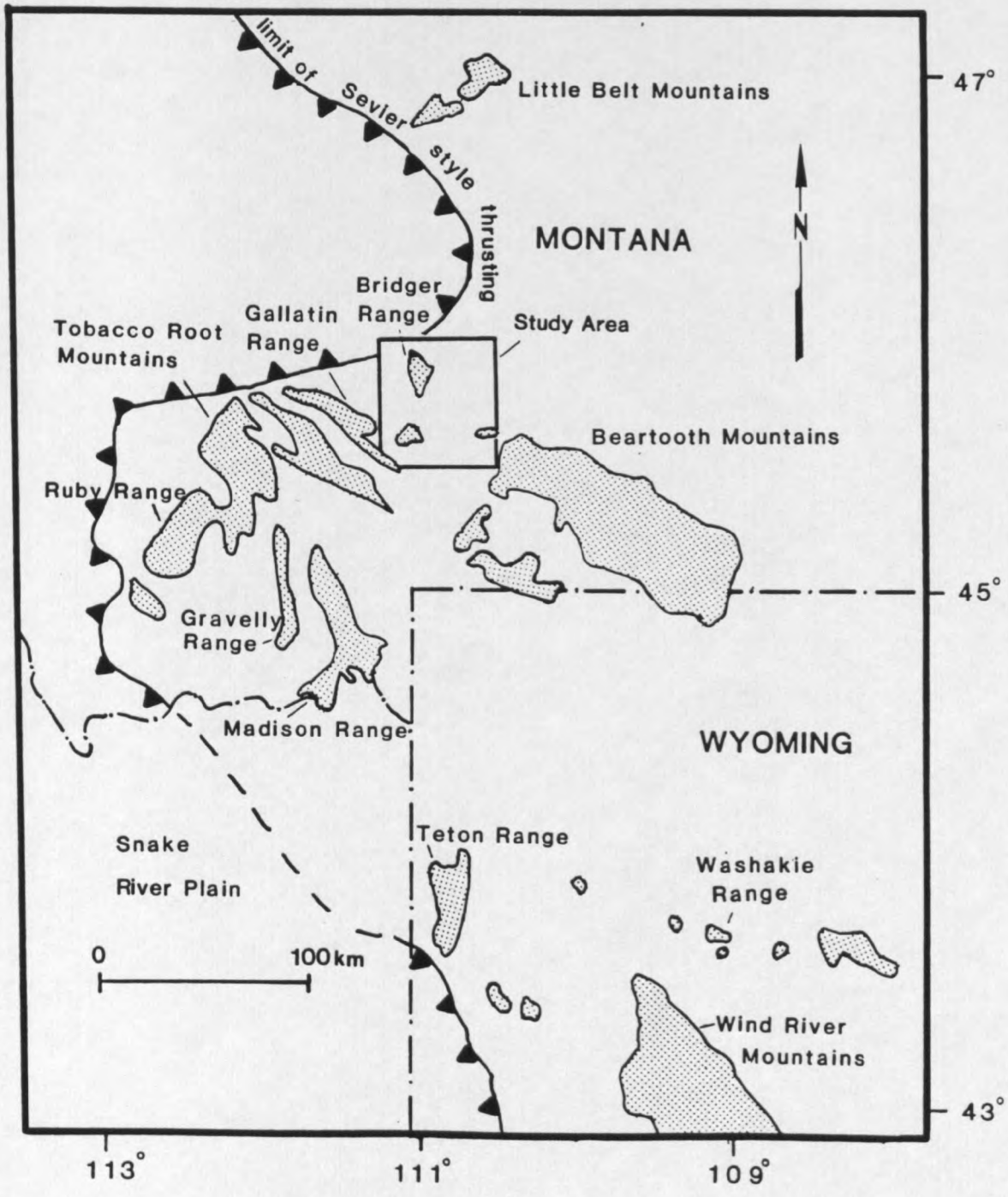

Figure 1. The northern Rocky Mountain foreland. Crystalline basement rocks are shown in stippled pattern. Inset is study area enlarged in Figure 2.

To a large degree, the debate over the fold and non-fold strain models stems from cross section construction techniques that model the basement experimentally without referencing field relations (Stearns, 1978; Erslev, 1986; Spang and Evans, 1985). To a lesser degree, it is due to equivocal exposures which lead to a myriad of interpretations (for example Elk Mountain, Wyoming: Blackstone, 1980 and Matthews, 1986; or Rattlesnake Mountain, Wyoming: Stearns, 1971 and Brown, 1984). In either case, inadequate field testing of these models on well exposed basement structures has sustained the controversy.

The Bridger and Gallatin Ranges of southwest Montana are Laramide-style uplifts with good exposures of basement rocks and sedimentary cover. These structures present an excellent opportunity to field test the fold and non-fold models. Differences between the models are found not only in the geometric configuration of the basement, but also in the movement history. Therefore, testing the validity of these models requires structural analysis of the geometric and kinematic elements on a mesoscopic and microscopic scale. These analyses will also constrain existing and future theoretical models of basement deformation.

During this field test, it was recognized that the pre-Laramide foliation attitude has a profound influence on the mechanical role of layering. Some foreland workers adamantly maintain that the layering plays no role in the rocks to be defined as "basement" (for example, Matthews, 1986). However, this is an artificial definition that clearly contradicts field evidence. Rather than having an arbitrary patchwork of basement - non-basement regions, it is appropriate to

consider all the metamorphic and igneous crystalline rocks of the Wyoming Province as "basement".

Study Area

The Bridger and Gallatin Ranges are located in the northern end of the Archean Wyoming Province (Engel, 1963)(Figures 1 and 2). These ranges are cored by weakly to well-foliated quartzofeldspathic gneiss, nonconformably overlain by Middle Cambrian sedimentary strata (Figure 3).

Southern Bridger Range

The Bridger Range, located immediately northeast of Bozeman, Montana, is an asymmetric, north-trending, east-verging, Precambrian-cored anticline with the west limb down-dropped by Cenozoic extension (Figure 2) (Lageson and Zim, 1985). The Ross-Pass fault zone, located in the central part of the range, separates Proterozoic Belt rocks to the north, from Archean metamorphic basement rocks to the south (Craiglow, 1986)(Figure 2). Thus, this zone has been inferred to be the south margin of Proterozoic Belt basin and thin-skinned thrusting in the Helena salient, and the north margin of Laramide basement-involved deformation (Craiglow, 1986, McMannis, 1955).

Gravity and seismic reflection data show that the basement of the southern Bridger Range has been thrusted 3 - 5 km over the Crazy Mountains Basin, producing a basement overhang (Lageson and Zim, 1985). Cenozoic extension on the west flank of the range produced a "perched

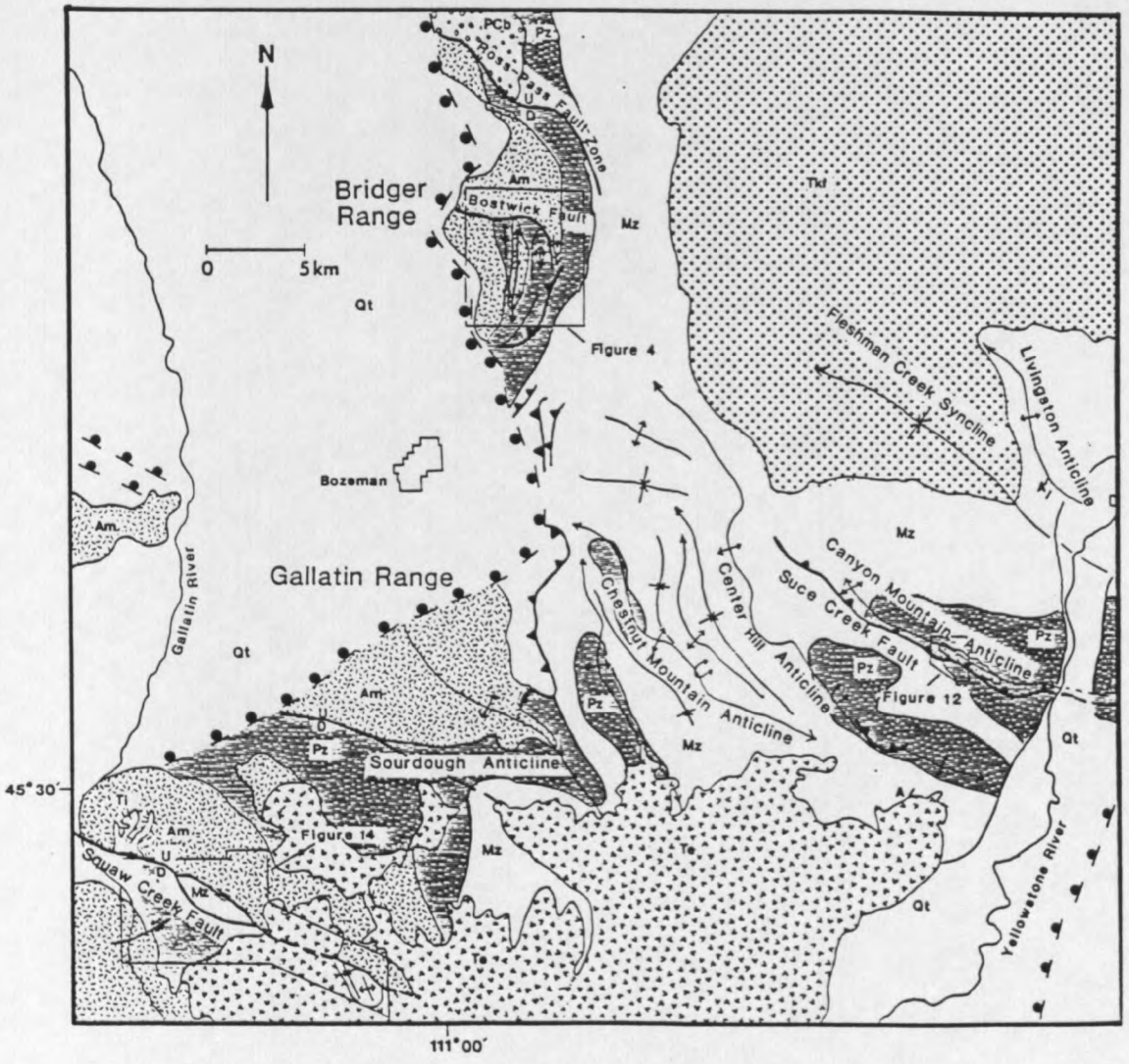

Figure 2. Major tectonic elements of the southern Bridger Range and northern Gallatin Range, Montana. Am - Archean metamorphic basement rocks; pCb - Precambrian Belt rocks; Pz -Paleozoic rocks; Mz - Mesozoic rocks; Tkf - Tertiary Fort Union Formation; Te - Tertiary extrusive rocks; Ti - Tertiary intrusive rocks; Qt - Quaternary alluvium (compiled from Roberts, 1972; Schmidt and Garihan; 1983; McMannis, 1955)

basement wedge" (Lageson and Zim, 1985). The perched basement wedge contains three, north-trending, basement-cored anticlines which developed along the crest of the larger, Laramide Bridger Range anticline (Figure 4). These folds are designated for reference as the western, central, and eastern anticlines (Figures 4). The western and central anticlines have excellent exposures of basement in their cores and were chosen for detailed study of basement behavior.

Northern Gallatin Range

The northern Gallatin Range is located immediately south of the Bridger Range. It is composed of several en echelon, northwest-trending folds that verge to the southwest (Figure 2). Many of these folds are bounded by northwest-striking contraction faults that dip northeast. Much of the range has been covered by Tertiary volcanic rocks which post-date Laramide deformation (McMannis and Chadwick, 1962) (Figure 2). A Late (?) Cenozoic normal fault truncates the north end of the range.

Squaw Creek fault, Sourdough anticline, Canyon Mountain anticline, and Suce Creek fault were selected for study based on exposure quality and structural significance. Squaw Creek fault is a major, northwest-trending Laramide reverse fault at the northwest corner of the range with good basement exposures along most of its length (Figure 2). Sourdough anticline, located in the north-central part of the range, is a large, northwest-trending, basement-cored anticline (Figure 2). A tear fault separates the tightly folded, northwest-trending nose of the fold from the north-trending, east limb (Figure 2). Poor exposures

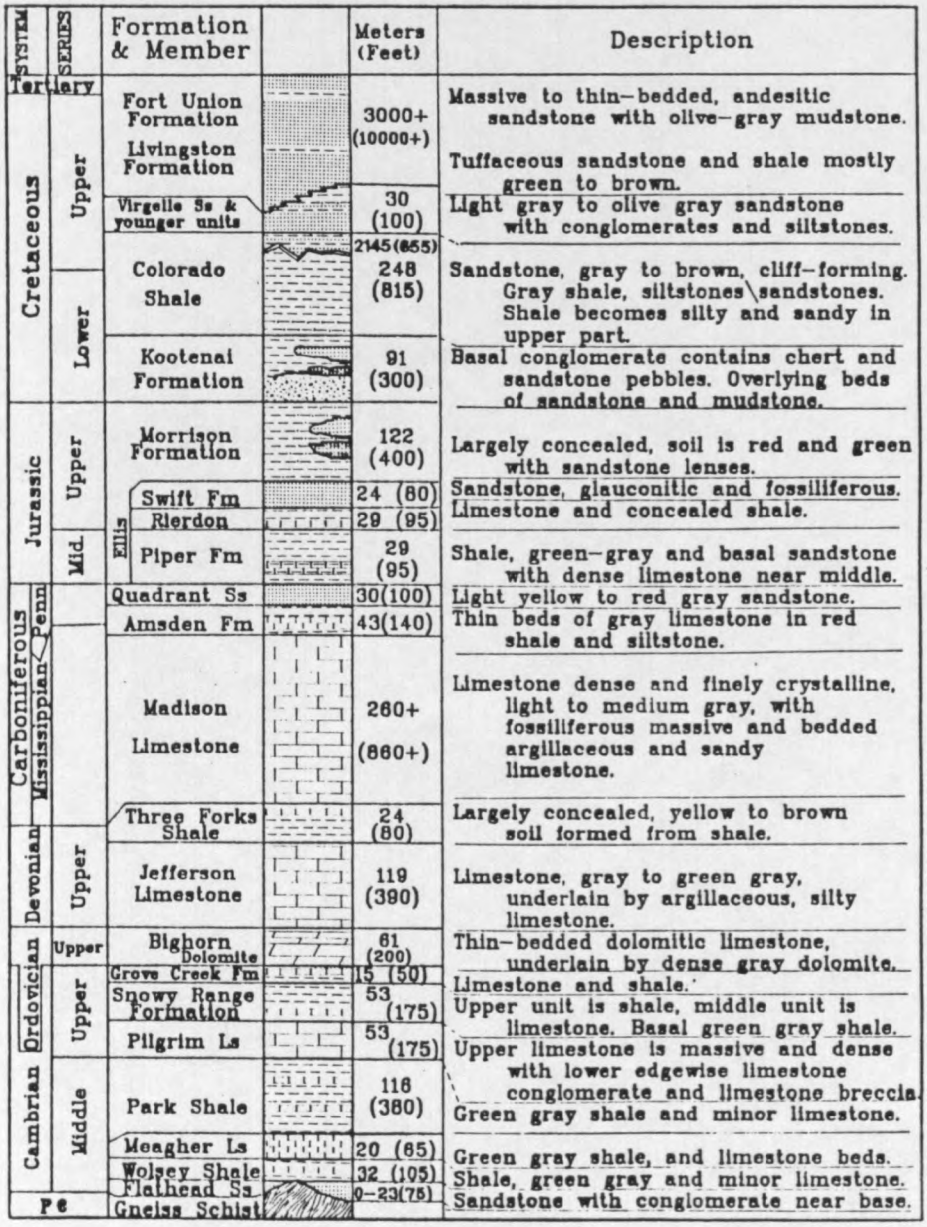

Figure 3 - Generalized stratigraphic column for the southern Bridger Range and northern Gallatin Range (from Robbins and Erslev, 1986; Richards, 1957; and Elliott and others, 1955).

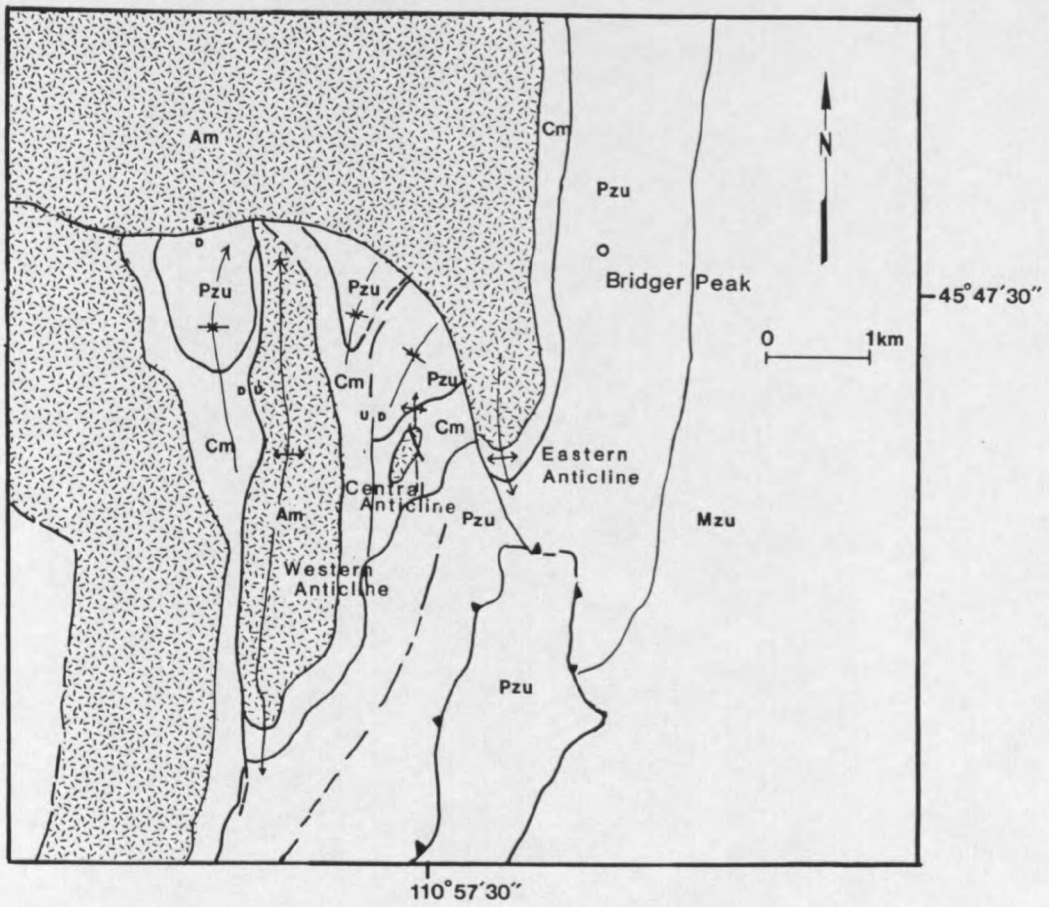

Figure 4. Geologic map of the study area in the southern Bridger Range. Location of map shown in Figure 2. Am - Archean metamorphic basement rocks; Cu - undifferentiated Cambrian rocks; Pzu - undifferentiated Paleozoic rocks; Mzu- undifferentiated Mesozoic rocks, (Geology from McMannis, 1955).

limited study of Sourdough anticline to the vicinity of the tear fault. Canyon Mountain anticline and Suce Creek fault are a northwest-trending, fold-fault pair located at the northeastern corner of the range (Figure 2). Canyon Mountain anticline lies in the hanging wall of Suce Creek fault and has good exposures of basement at its northwest end.

Methods of Investigation

The methodology used in this field test of Laramide basement strain models involves an analysis of geometric and kinematic elements. Comparisons of pre-Laramide structures in the basement were made with Laramide structures in the overlying Phanerozoic section to determine which fabrics in the basement result from Laramide deformation as opposed to Archean or Proterozoic deformation. These structural analyses were then used to evaluate the fold and non-fold strain models.

Geometry

To establish basement geometry, the orientation of pre-Laramide foliations and lineations were mapped in the field. These penetrative metamorphic features have been inferred by radiometric age dates (2700 m.y.) to have formed during Archean amphibolite to granulite grade metamorphism (James and Hedge, 1980). The attitude of Cambrian strata was then mapped and used for control of Laramide geometry.

Orientations of pre-Laramide structures were plotted on equal area, lower hemisphere, stereographic projections and reviewed for a consistent relationship with respect to the Paleozoic strata. Thus, the Laramide basement fabric was established from its geometrical relationship to the overlying Cambrian strata.

Kinematics

The orientation, offset, and slip direction for each mesoscopic fault mapped was recorded. These striated and grooved fault surfaces

provide a succinct kinematic record of deformation (Price, 1966). Each fault defines a unique line of slip, an axis of rotation (b kinematic axis), and a direction of shortening or extension.

The b kinematic axis (or axis of rotation) is defined as the line which lies on the plane of the fault and is perpendicular to the slip direction (Price, 1966). In monoclinic structures, such as the asymmetric, concentric, Laramide folds in Paleozoic strata (Schmidt and Garihan, 1983), the b kinematic direction for the fold is parallel to the fold axis (Wilson, 1982, p. 12-15). The fold axis orientation was determined by locating the pole (fold axis or pi pole) to the great circle defined by poles to bedding (pi circle). Based on this relationship, an axis of rotation for Laramide deformation was established. Collective consideration of b kinematic directions from Paleozoic folds and slickensided fault surfaces documents the kinematics of basement rocks during Laramide deformation.

The possibility that movement on mesoscopic faults represents Cenozoic extension is unlikely since Paleozoic folds can be continuously traced without any disruption by extensional faults. Furthermore, as will be shown in Chapter 3, the mean b kinematic direction determined from basement faults was subparallel to the b kinematic axis of the Laramide fold, indicating that deformation of basement rocks and Paleozoic strata was coeval.

Influence of foliation attitude on Laramide basement response was determined by rotating foliations into their pre-Laramide positions. This was accomplished by stereographically unfolding the Phanerozoic section into a horizontal, pre-Laramide attitude. The same rotation

was performed for the corresponding basement rocks, placing them in a pre-Laramide orientation. However, horizontal Laramide rotations may have affected the basement rocks. Therefore, only the pre-Laramide foliation dip can be known with certainty.

For a given structural domain, the pre-Laramide foliation attitude was correlated to Laramide basement response (fold or non-fold). These correlations provide evidence for the effects of foliation attitude on Laramide deformation.

Shear Zone Deformation

The microscopic mechanisms by which Laramide strains were accommodated has received little attention. However, the role of fluids, finite strain, and strain rate may have varied significantly within the Laramide structural province. Thus, petrographic studies were made on twenty-five oriented thin sections from Laramide shear zones. Mineralogical and textural observations were used to determine processes of deformation, retrograde mineralization, and pressure and temperature conditions. Results of these investigations were then compared to other studies of Laramide shear zones.

The proximity of the field area to the south margin of the Belt basin presented the possibility that the basement rocks were affected by a Proterozoic greenschist retrograde event. Therefore, shear zone analysis was limited to zones which show a clear geometric and kinematic relationship to Laramide deformation.

Models of Foreland Uplifts

The established geometric and kinematic relations were used to evaluate the fold and non-fold models for Canyon Mountain anticline, Squaw Creek fault and the Bridger Range. Other field investigations of basement-cored anticlines in Wyoming, Colorado and New Mexico were integrated with this study to establish a mechanical framework for basement deformation in the fold model.

Archean Lithology and Deformation

The predominant Archean lithology in the study area is weakly to well- foliated, quartzofeldspathic gneiss. Amphibolite is present as boudins, lenses, and thin, foliation-parallel layers within the quartzofeldspathic gneiss. Quartz and pegmatite dikes cross-cut the quartzofeldspathic gneiss and amphibolite.

At least two styles of ductile folding are present in the Archean metamorphic rocks. The first style is characterized by tight to isoclinal folds with axial-planar foliation. The second fold style is characterized by open folds. These folds refold isoclinal folds. Therefore, tight to isoclinal folds are designated F1 and Archean open folds are designated F2. Wavelengths of F1 and F2 folds range from a few centimeters to tens of meters. Open folds on a kilometer scale are present south of Squaw Creek fault in the Gallatin River Canyon. However, presence of these folds was impossible to determine in the field area because of Laramide foliation rotation.

STRUCTURAL GEOMETRY

As will be shown in this chapter, basement folding accompanied folding of Paleozoic rocks in the southern Bridger Range and Canyon Mountain anticline. At Squaw Creek fault, however, there is no evidence of basement folding.

Fold Style of Paleozoic Rocks

A near-cylindrical geometry for the Paleozoic folds investigated is indicated by the narrow width of the pi circles (less than 20° scatter)(Davis, 1984)(Figures 5a, 6a, and 6b). In addition, folds in the structurally dominant Meagher Limestone are open and concentric and have broad hinge zones. Interlimb angles range from 90° in the western syncline, Bridger Range to 110°, in the central anticline, Bridger Range (Figure 6). The Pilgrim Limestone exhibits the same geometry as the Meagher Limestone except at Canyon Mountain anticline, where the Pilgrim Limestone is tightly folded with an interlimb angle of 40°. The Meagher Limestone in this fold is cut by Suce Creek fault and shows an interlimb angle of 100°. Cambrian shales are significantly thickened in the hinge zone of the central anticline, Bridger Range (Figure 6) and are considerably thinned on the overturned, detached limb of Canyon Mountain anticline indicating a similar fold geometry.

Southern Bridger Range

Western Anticline: Paleozoic Geometry

Fold axes of the three anticlines within the "perched basement wedge" of the Bridger Range trend to the north (Figure 4). The fold axis for the south end of the western anticline, determined from Cambrian Meagher Limestone bedding, has a shallow plunge to the south and parallels the range trend (Figure 5a). The adjacent syncline has a fold axis with a similar trend and was used for control of Laramide geometry at the north end of the western anticline (Figure 5b).

Central Anticline: Paleozoic Geometry.

The central anticline of the southern Bridger Range is geometrically unique. In the core of an open fold of Meagher Limestone are two anticlines of Flathead Sandstone with the adjoining limbs truncated by a high-angle, reverse fault (Figure 6). The fault dies out into a thickened section of Wolsey Shale. The slightly skewed orientation between the Meagher fold axis (Figure 6a) and the fold axis from the Flathead Sandstone (Figure 6b) is attributed to a minor detachment occurring in the Wolsey Shale.

Central and Western Anticlines: Basement Geometry

Planar Structures. Fold axes, determined from basement foliation surfaces in the western and central anticlines, are approximately coaxial with the fold axes determined from Paleozoic strata (Figures 5 and 6). This suggests that Archean metamorphic

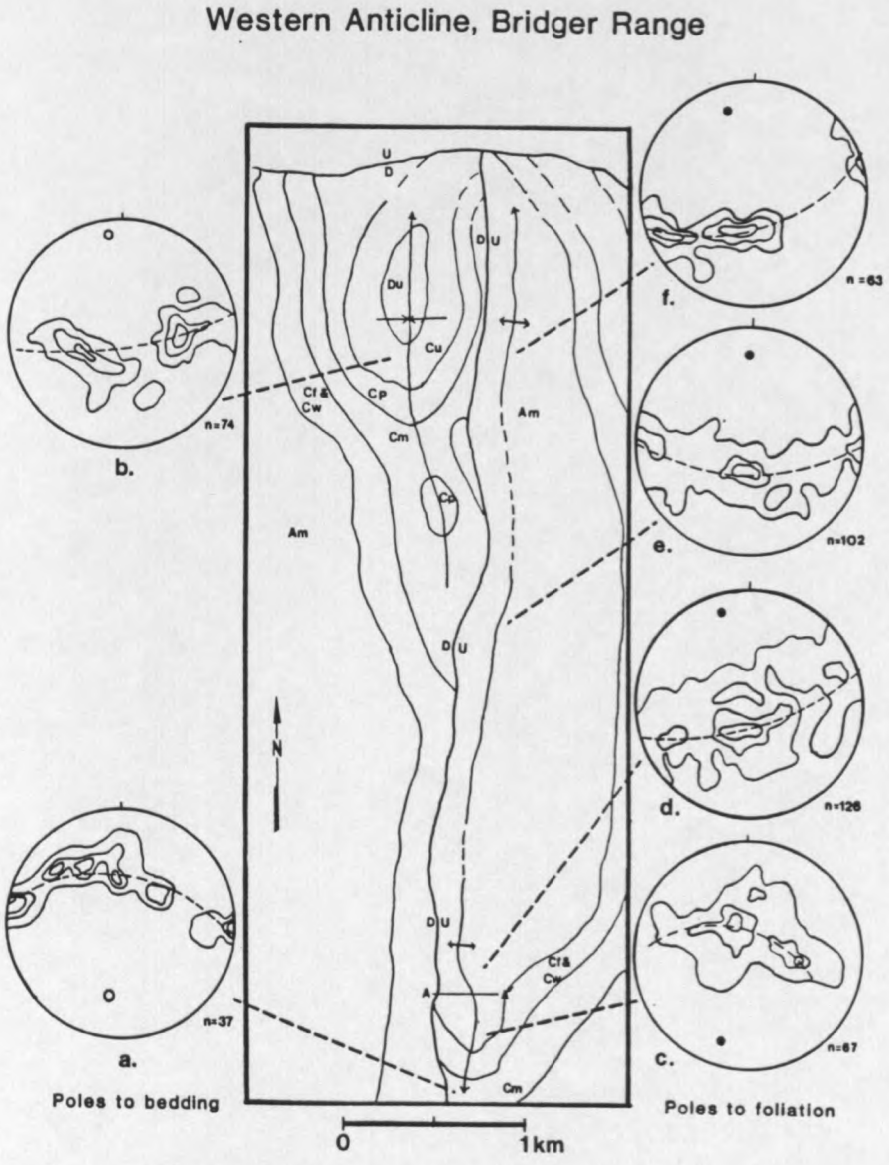

Figure 5. Fold geometry of the western anticline, Bridger Range. Fold axes determined from Archean metamorphic foliation surfaces are coaxial with fold axes determined from Paleozoic bedding. Equal area, lower hemisphere, stereographic projections. a) Poles to Cambrian Meagher Limestone bedding. b) Poles to Cambrian Pilgrim Limestone bedding. c) Poles to foliation from upper basement surface indicate conical folding. d-f) Poles to Archean metamorphic foliation. Line A-A' is line of photograph (Figure 7) and line diagram (Figure 22). Contour interval is 0, 5, 10, and 15% per 1% area. Am - Archean metamorphic rocks; Cf - Flathead Sandstone; Cw - Wolsey Shale; Cm - Meagher Limestone; Cp - Park Shale; Cu - Upper Cambrian undivided; Du - Devonian undivided.

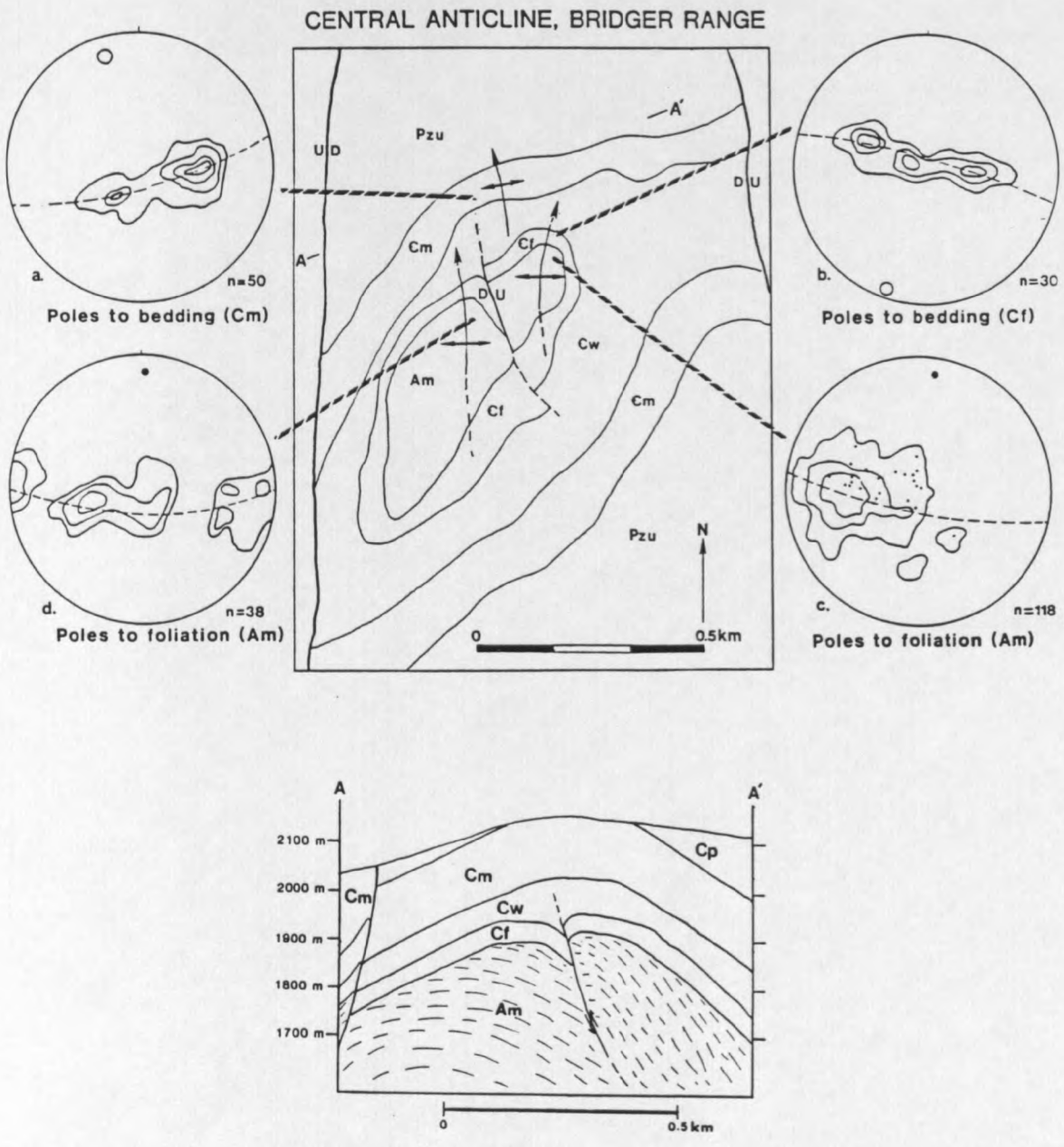

Figure 6. Fold geometry of the central anticline, Bridger Range. Fold axes determined from foliation surfaces are coaxial with fold axes of the Paleozoic rocks. A-A' is line of cross section. Equal area, lower hemisphere, stereographic projections. a) Poles to Meagher Limestone bedding. b) Poles to Flathead Sandstone bedding. c) Poles to basement foliation. Solid dots are from stations within 20 m of upper basement surface. d) Poles to basement foliation. Am - Archean metamorphic rocks; Cf - Flathead Sandstone; Cw - Wolsey Shale; Cm - Meagher Limestone; Pzu - undivided Paleozoic rocks. Contour interval is 0, 5, 10, and 15% per 1% area.

foliation surfaces were folded into parallelism with Paleozoic bedding (Figures 7 and 8). Thus, the geometry of these anticlines fits the "fold" model of basement deformation proposed by Berg (1962) and Schmidt and Garihan (1983). Field photographs of these anticlines reveal the folded basement (Figures 7 and 8).

Geometric analysis of basement folds suggests that a transition from conical folds to cylindrical folds occurs with increasing distance down section from the upper basement surface. The angle of discordance between Archean metamorphic foliation surfaces and the Cambrian Flathead Sandstone is low (10°-15°). The linear intersection of the foliation surfaces with the Flathead Sandstone is approximately perpendicular to the Laramide fold axis (Figure 9). This represents a special arrangement where the angle of discordance (δ) will remain constant throughout cylindrical folding of the Paleozoic cover (Figure 9)(Ramsay, 1967, p. 496). The result is conical folding of the upper basement surface (Figures 5c, 6c, and 9).

The loci of poles to foliation at the south end of the western anticline are concentrated about a small circle that corresponds to a conical fold in the upper basement surface (Figure 5c). The cone axis is parallel to the fold axis defined by poles to bedding (Figure 5a). The conical form gives way to cylindrical folding in structurally lower levels to the north (Figures 5d, 5e, and 5f). Above and below the zone of transition the basement and cover rocks deform independently. An analogous transition zone has been noted at Big Thompson anticline, Colorado (LeMasurier, 1970) and is discussed in Chapter 5.

Figure 7. View of the basement core, western anticline, Bridger Range, looking north. Dark lines show foliation surfaces. Line of photograph is along east half of Line A-A', Figure 5. Line sketch of diagram is shown in Figure 22. Arrow indicates location of Figure 23.

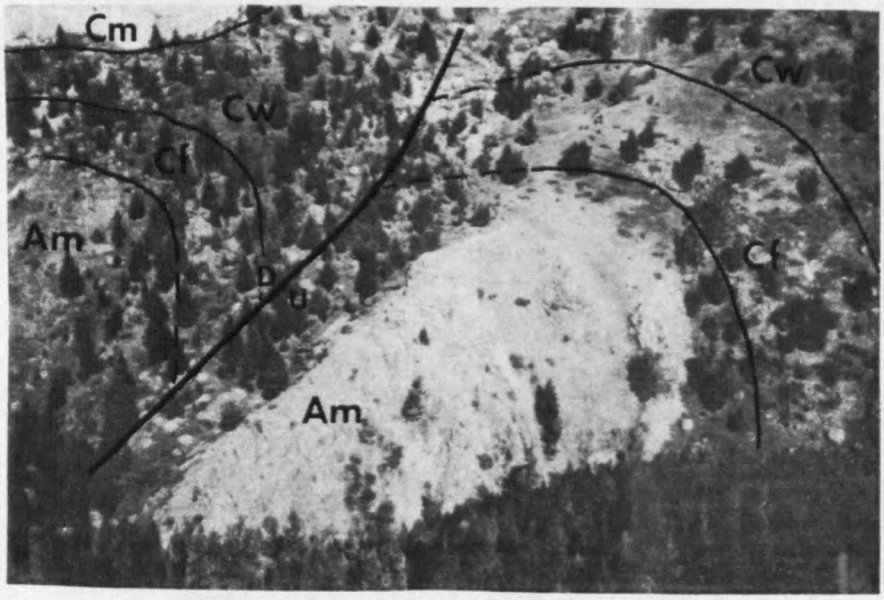

Figure 8. View of the eastern segment of the central anticline, Bridger Range, looking northwest. Fold axis parallels top of treeless ridge. Dark lines show foliation surfaces in basement. High angle reverse fault separates folded basement segments on west (left) side of ridge. Cm - Meagher Limestone; Cw - Wolsey Shale; Cf - Flathead Sandstone; Am - Archean metamorphic rocks.

The geometry of the upper basement surface is equivocal in the central anticline (Figure 6c, solid dots). However, at lower stuctural levels, the loci of poles to foliation fall along a great circle indicating a cylindrical geometry (Figures 6c, contour lines and 6d).

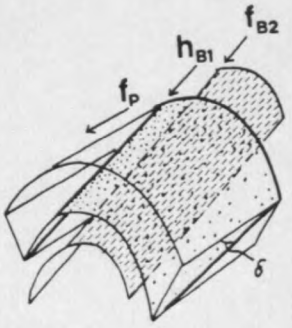

Figure 9. Idealized geometric arrangement of basement and sedimentary cover for western and central anticlines. f_p - fold axis to cylindrical fold in Cambrian rocks; h_{B1} - hingeline to conical fold in upper basement surface; f_{B2} - fold axis to cylindrical fold in lower basement; gamma - angle of discordance between Cambrian Flathead Sandstone and basement foliation surfaces; Note intersection of upper basement surface (stippled pattern) with base of Cambrian rocks is perpendicular to Laramide fold axis (modified from Ramsay, 1967).

Linear Structures. The fold axes of Archean F1 and F2 folds from the western anticline are plotted in Figure 10. If the F1 and F2 Archean folds were coaxial in their pre-Laramide position, then the hingelines should be distributed around a small circle such that the angle between the Archean fold hinges and the Laramide fold axis remained constant (Ramsay, 1967, p. 463). However, fold axes show a wide scatter with a maximum which is subparallel to the Laramide fold axis (Figure 10). Variation from the maximum indicates either: 1) a non-coaxial arrangement prior to Laramide deformation or 2) Laramide rotation of macrogranular blocks (Chapter 3) about axes oblique to the

Laramide fold axis. The former interpretation is favored based on the large number of fault rotation axes that parallel the Laramide fold axis (Chapter 3).

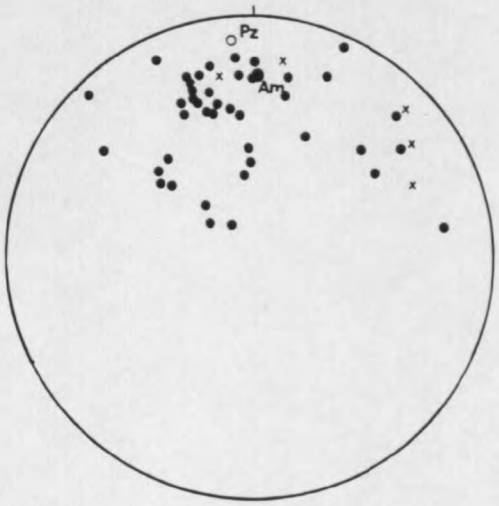

Figure 10. Archean fold axes from the western anticline. Data are from the same domain as Figure 5d. Crosses - tight to isoclinal F1 folds; Solid dots - open F2 folds.

Eastern Anticline

Paleozoic Geometry. The fold axis of the eastern anticline parallels the trend of the central anticline, but has a moderate plunge to the south (Figure 11a).

Basement Geometry. Poor exposures of basement rocks in the core of the eastern anticline make determination of geometry equivocal. A plot of poles to foliation show two, steeply dipping, north-striking populations (Figure 11b). The Laramide geometry of the eastern anticline may be interpreted as either undeformed rigid basement or as non-rigid, folded basement where the crest of the fold is not exposed. The latter interpretation is favored in view of the similar lithology of this anticline to the central and western anticlines.

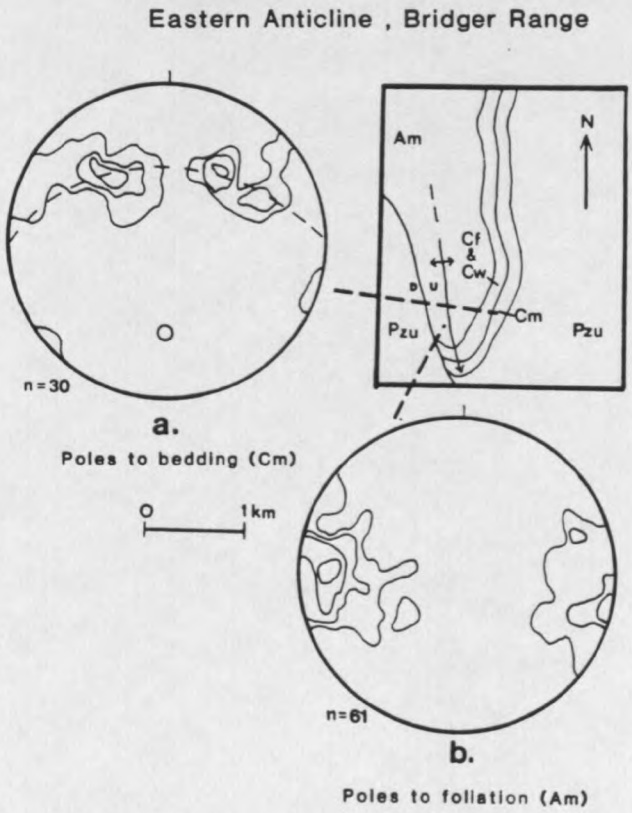

Figure 11. Fold geometry of the eastern anticline, Bridger Range. Equal area, lower hemisphere, stereographic projections. a) Poles to Meagher Limestone bedding. b) Poles to basement foliation surfaces. Am - Archean metamorphic rocks; Cf - Flathead Sandstone; Cw - Wolsey Shale; Cm - Meagher Limestone; Pzu - undifferentiated Paleozoic rocks. Contour interval is 0, 5, 10, and 15% per 1% area.

Northern Gallatin Range

Canyon Mountain Anticline

Paleozoic Geometry. Canyon Mountain anticline lies on the hanging wall of Suce Creek fault and verges to the southwest. Suce Creek fault has a minimum stratigraphic displacement of 1273 meters where basement rocks are thrusted over Cretaceous Kootenai Formation (Roberts, 1972) The fault has a moderate dip to the northeast and strikes northwest (305; 45 NE). The fold axis for Canyon Mountain

anticline, defined by the Flathead Sandstone, trends northwest, parallel to the map trace of Suce Creek fault (Figure 12a). The southwest limb of Canyon Mountain anticline is vertical to overturned and contains shale units that are noticeably thinned.

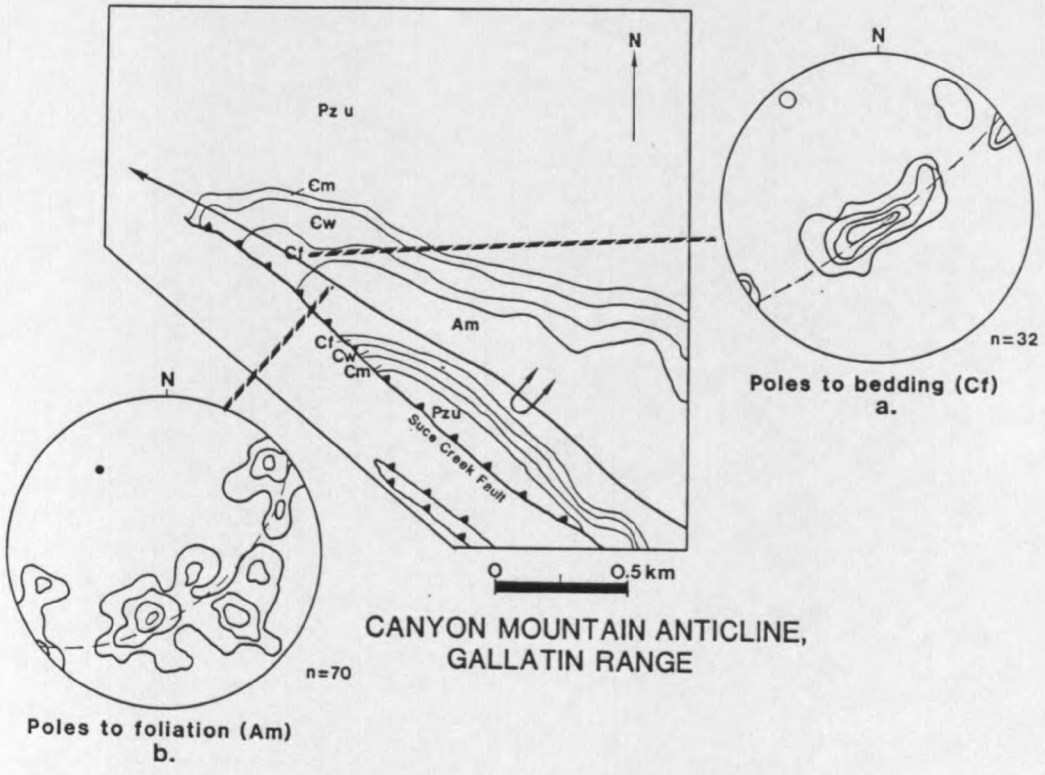

Figure 12. Fold geometry at Canyon Mountain anticline, northeastern Gallatin Range. Location shown in Figure 2. Fold axes determined from basement foliation surfaces are coaxial with fold axes determined from Paleozoic bedding surfaces. Equal area, lower hemisphere, stereographic projections. a) Poles to Flathead Sandstone bedding. b) Poles to basement foliation surfaces. Contour interval is 0, 5, 10, and 15% per 1% area. Am - Archean metamorphic rocks; Cf - Flathead sandstone; Cw - Wolsey Shale; Cm - Meagher Limestone; Pzu - undifferentiated Paleozoic rocks.

Basement Geometry. The fold axis determined from basement foliation surfaces at Canyon Mountain anticline is coaxial with the Paleozoic fold axis (Figure 12b). This relationship indicates the basement at Canyon Mountain anticline was also folded into parallelism with the overlying Paleozoic rocks. This can be clearly seen in an aerial photograph of Canyon Mountain anticline where a distinctive amphibolite layer folds conformably with the overlying strata (Figure 13). Partial exposures precluded detailed investigation of fold geometry for the upper basement surface.

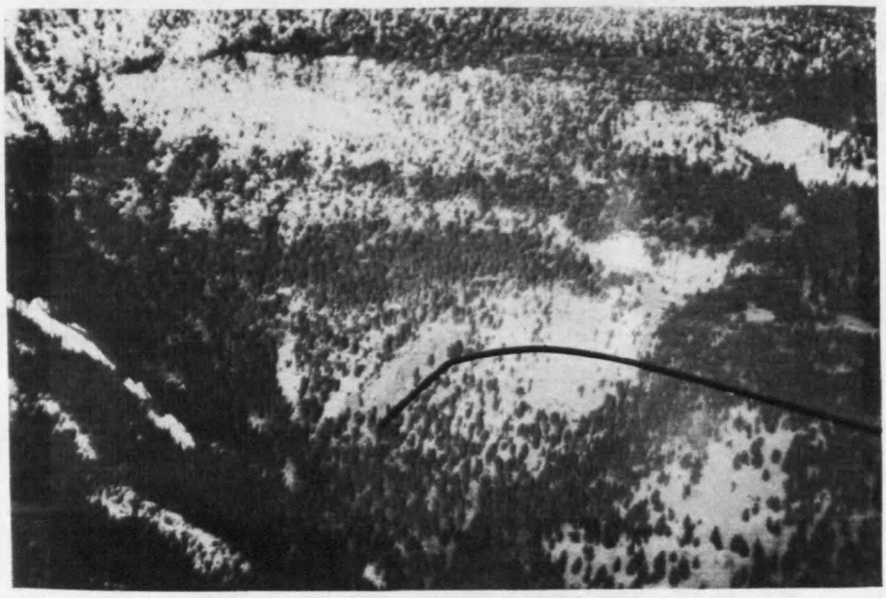

Figure 13. Aerial photo of Canyon Mountain anticline looking north. Prominent ridge in background is Mississippian Madison Group Limestone on the northeast limb of the fold. A prominent amphibolite layer strikes northeast in the nose of the fold.

The loci of poles to foliation surfaces in the central, western, and Canyon Mountain anticlines show a wider dispersion about the pi circle than was recognized in the Paleozoic rocks. Ramsay (1967) noted that the symmetry of the final product of deformation is a combination of the kinematic and original fabrics. Therefore, the final product

generally represents a lower order of symmetry. The scatter of poles to foliation is explained by two episodes of superimposed, Archean folding overprinted by Laramide folding (Figure 10).

Squaw Creek Fault

Paleozoic Geometry. Squaw Creek fault, located in the northwestern Gallatin Range, has a northwest-trend similar to Suce Creek fault, but dips more steeply (314; 80 NE) (Figure 14). Tertiary volcanic rocks cover the central portion of the fault and divide it into two exposed segments. The southeastern portion is referred to as the "Timber Butte segment" and the longer, northwest exposure of the fault is designated the "northwest segment". Minimum stratigraphic displacement of 1455 meters is evidenced by basement rocks placed over Cretaceous Colorado Group rocks (McMannis and Chadwick, 1964). Imbricate faulting in the hanging wall takes up displacement at the southeast end of the northwest segment (Figure 14).

The geometry of Paleozoic rocks at Squaw Creek fault is characterized by planar, shallow-dipping strata. The footwall of Squaw Creek fault is comprised of planar, shallowly-dipping strata, cut by numerous north to northeast-trending faults (Figure 14). The only exception to this geometry are two small, northwest-trending, en echelon folds in Mississippian strata, truncated obliquely by Squaw Creek fault (Figure 14c, open circles). With the exception of an outlier of shallow dipping Cambrian rocks, Paleozoic rocks are absent from the hanging wall. The Flathead Sandstone, which overlies exposed basement in the imbricate slice, is planar and subhorizontal (Figure

14b). Immediately adjacent to the fault, disharmonic folds are present in the Meagher Limestone indicating a minor detachment in the Wolsey Shale.

Basement Geometry. Basement geometry in the Squaw Creek area is in marked contrast to the configuration identified in the southern Bridger and northeastern Gallatin Ranges. The geometry is characterized by foliation with a steep dip and either north to northeast strike (northwest segment)(Figures 14a, 14d, and 14e) or northwest strike (Timber Butte segment)(Figure 14c, solid circles).

Absence of rotated foliations and the planar Flathead-Archean contact indicate that basement in the vicinity of Squaw Creek fault behaved in a rigid manner. The contrast between basement behavior at Squaw Creek fault and other structures in the study area results from different pre-Laramide foliation attitudes, as discussed in the following chapter.

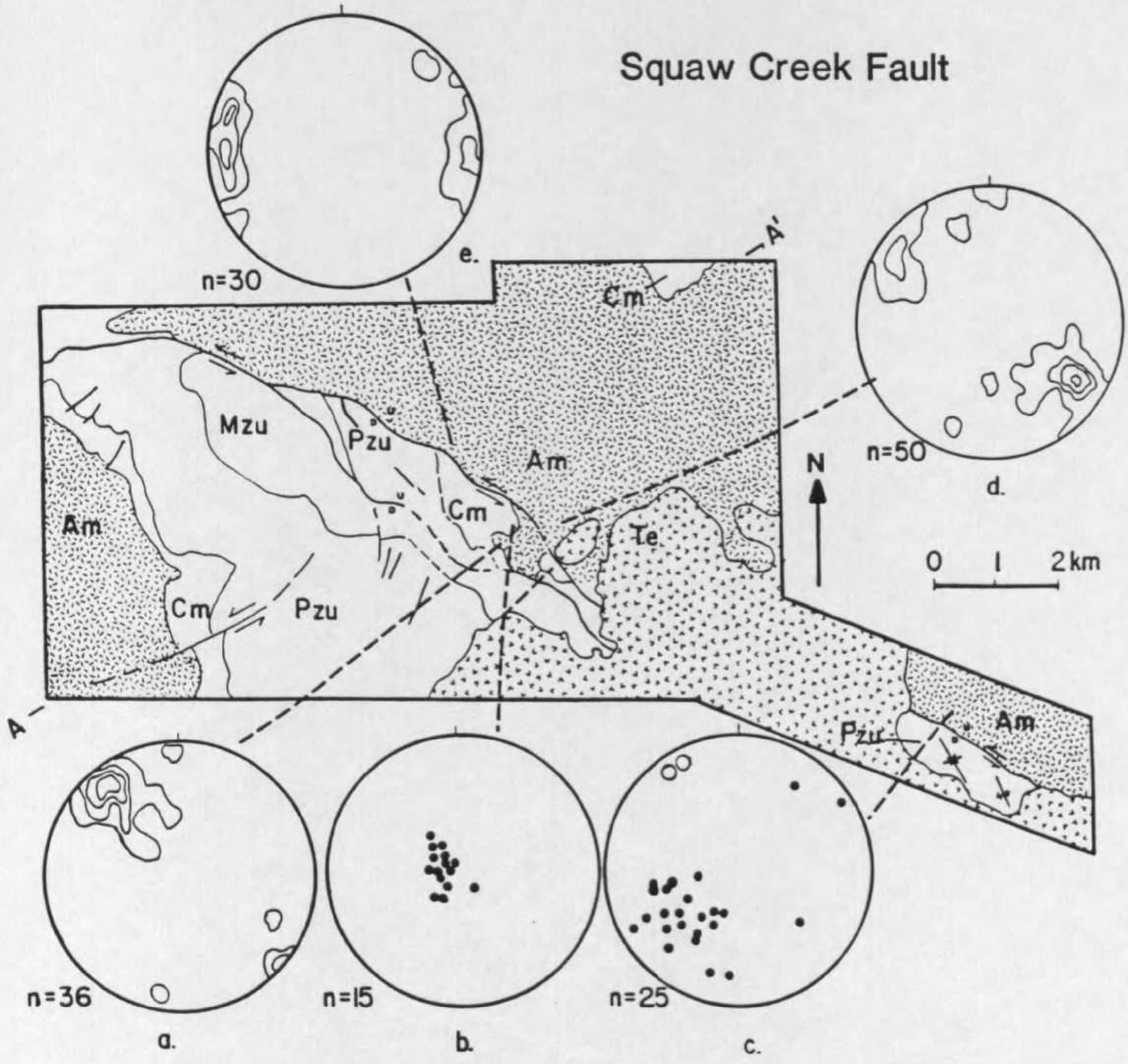

Figure 14. Structural geometry along Squaw Creek fault. Location shown in Figure 2. With the exception of two folds in the Timber Butte segment, Paleozoic strata are planar. Equal area, lower hemisphere, stereographic projections. a) Poles to foliation. b) Poles to Flathead Sandstone bedding c) Open circles - Fold axes to Mississippian strata; solid dots - poles to Archean metamorphic foliation. d and e) Poles to basement foliation. Am - Archean metamorphic rocks. Cm - Middle Cambrian rocks; Pzu - undifferentiated Paleozoic rocks; Mzu - undifferentiated Mesozoic rocks. Contour interval is 0, 5, 10, and 15% per 1% area (geology from McMannis and Chadwick, 1964).

MECHANISMS OF LARAMIDE BASEMENT DEFORMATION

Control of Pre-Laramide Foliation

The orientation of foliation surfaces exerted a fundamental control on basement response to Laramide deformation in the study area. Except at Squaw Creek, Precambrian foliation surfaces have been folded into parallelism with the overlying Paleozoic strata. Restoration of folded foliation surfaces to their pre-Laramide orientation yields a subhorizontal attitude (Figure 15). The pre-Laramide dip ranges from 10° in the western anticline to 24° at Canyon Mountain anticline. At Squaw Creek fault, however, Laramide basement folding was absent and the restored foliation dips 70°-80° (Figure 15).

In regions where folds developed, the subhorizontal foliation surfaces provided a path of low shear strength. As the kinematic indicators presented later in this chapter suggest, the subhorizontal foliation surfaces allowed the basement to shorten by flexural-slip folding along foliation-parallel surfaces.

Correlation of shallow-dipping, pre-Laramide surfaces with Laramide folds indicates that orientation of foliation controlled the basement response. Application of this axiom to the poorly exposed Sourdough anticline explains the presence of the tear fault along its east limb (Figure 2). This fault separates the tightly folded, northwest-trending segment of the anticline from the openly folded, north-trending, east limb (Figures 2 and 15). Rotation of foliation into

their pre-Laramide orientation indicates a subhorizontal attitude in the core of the fold and a near vertical attitude along the east limb. Thus, the fault is attributed to differential shortening due to a structural transition within the basement.

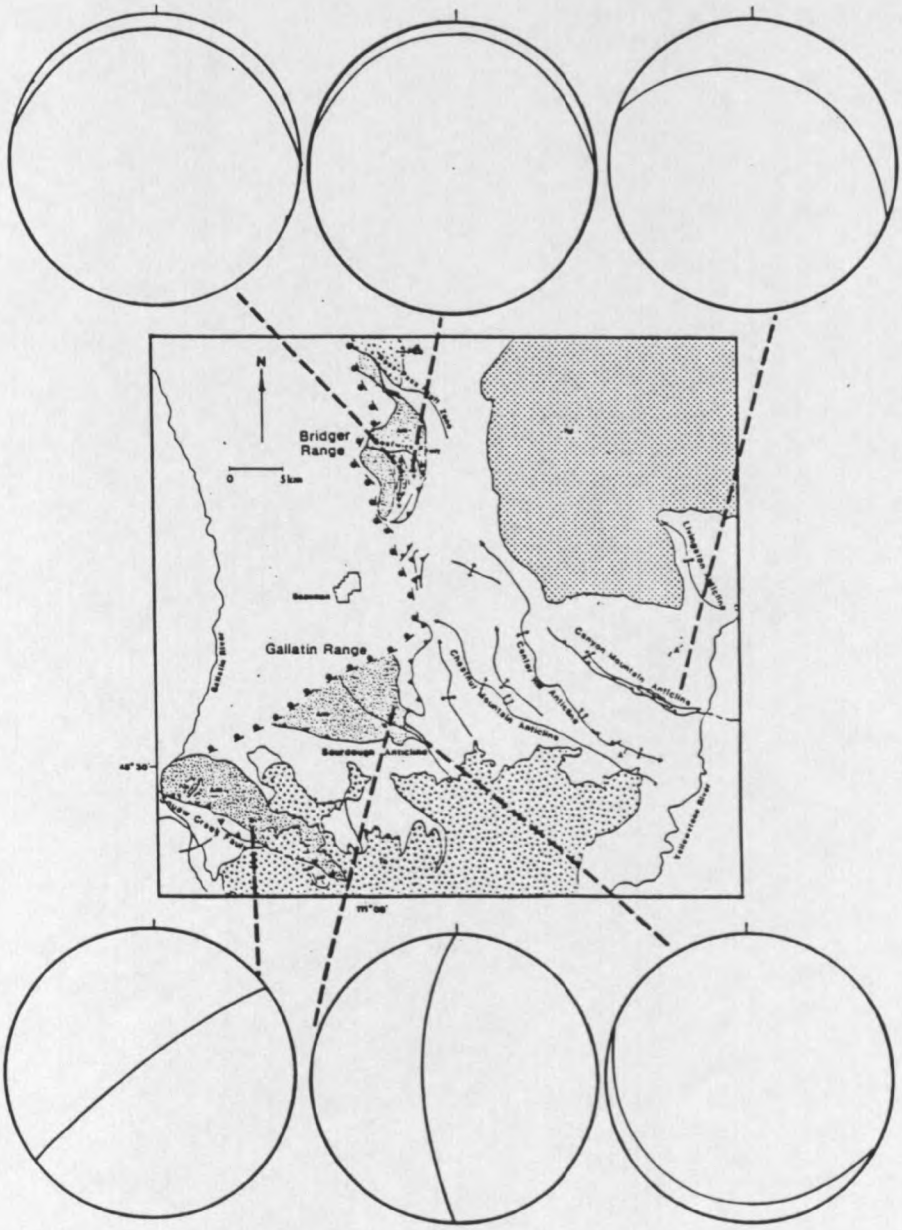

Figure 15. Average pre-Laramide foliation orientation for the northern Gallatin Range and southern Bridger Range, Montana. Subhorizontal foliation surfaces correspond to regions of folded basement.

Fold Kinematics

Slickensided and striated fault surfaces reflect the displacements, rotations and distortions of basement rocks during folding. In this section, analysis of these mesoscopic subfabrics will provide evidence that the basement deformed predominantly by oblique, flexural-slip with lesser amounts of passive-slip (Donath and Parker, 1964). Passive-slip occurred in regions where Archean folds blocked foliation-parallel glide planes. Large, internally undeformed, basement blocks indicate a significant amount of deformation was accomplished by macrogranular rotation and translation. These elements of deformation are considered in detail below.

Foliation-Parallel Faults

Slickenside striations measured on foliation-parallel shear surfaces from the western and Canyon Mountain anticlines are symmetric about their fold axes (Figure 16). Symmetry of these slickensides about the Laramide axis of rotation indicates they formed in concert with Laramide folding of overlying strata. In the ideal case for cylindrical, flexural-slip folds, slickenside lineations lie on the pi circle of the fold, perpendicular to the fold axis (Figure 16, dashed great circles)(Donath and Parker, 1964). However, slickenside lineations for these anticlines plunge more steeply than the ideal case in the direction of pre-Laramide foliation dip (Figures 15 and 16). Therefore, a component of simple shear occurred between foliation surfaces, parallel to the fold axis. This mechanism of folding has

been termed oblique flexural-slip (Ramsay, 1967)(Figure 17). Oblique flexural-slip folds have been documented in other cases where rock layers are inclined to the bulk strain axes (Ramsay, 1967, p. 396; Wilson, 1982, p. 19).

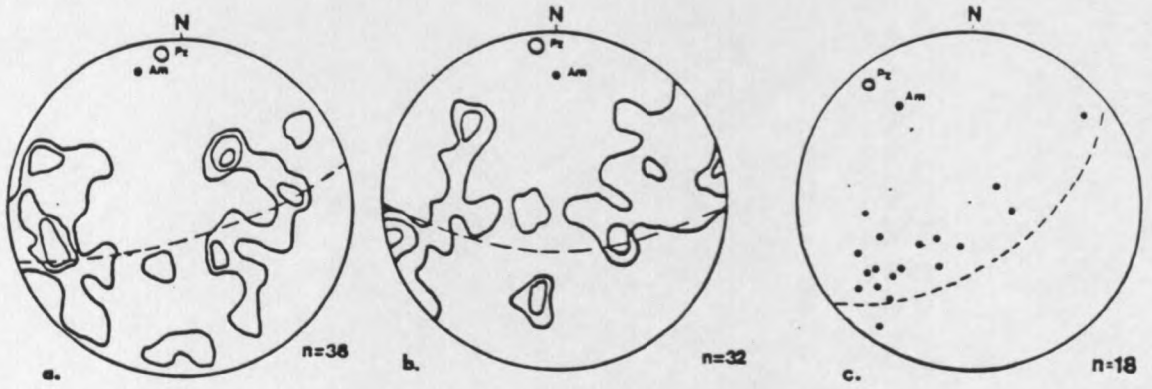

Figure 16. Slickenside lineations measured along foliation-parallel surfaces. a) Western anticline, from same domain as figure 5d. b) Western anticline, from same domain as figure 5e. c) Canyon Mountain anticline. Open circles are Paleozoic fold axes. Solid circles are basement fold axes. Contours are 0, 5, 10, and 15 % per 1 % area.

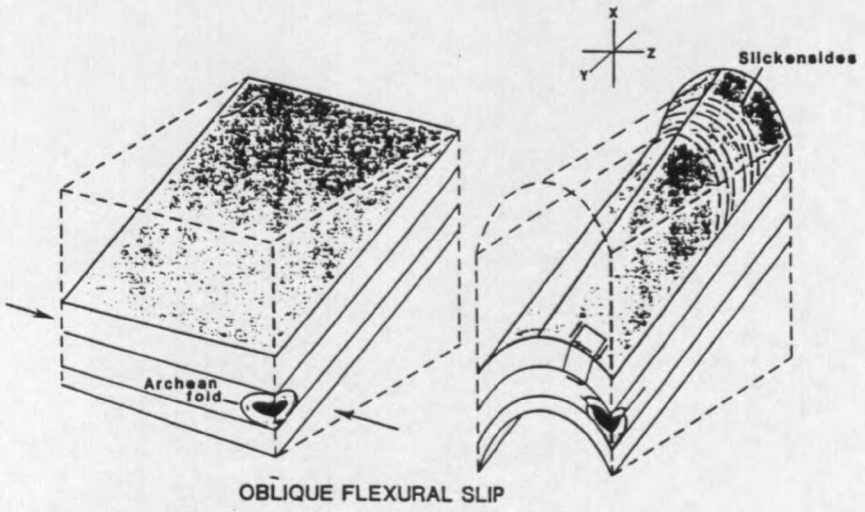

Figure 17. The oblique flexural slip mechanism. a) Pre-Laramide foliation surfaces have a shallow dip. b) Oblique flexural slip results in a component of simple shear parallel to the fold axis (Modified from Ramsay, 1967, p. 396).

Foliation-Oblique Faults

A discontinuous system of mesoscopic, foliation-oblique faults is present in the basement of the western, central, and Canyon Mountain anticlines. b kinematic directions for these fault sets parallel the Laramide fold axis, indicating coeval movement (Figure 18).

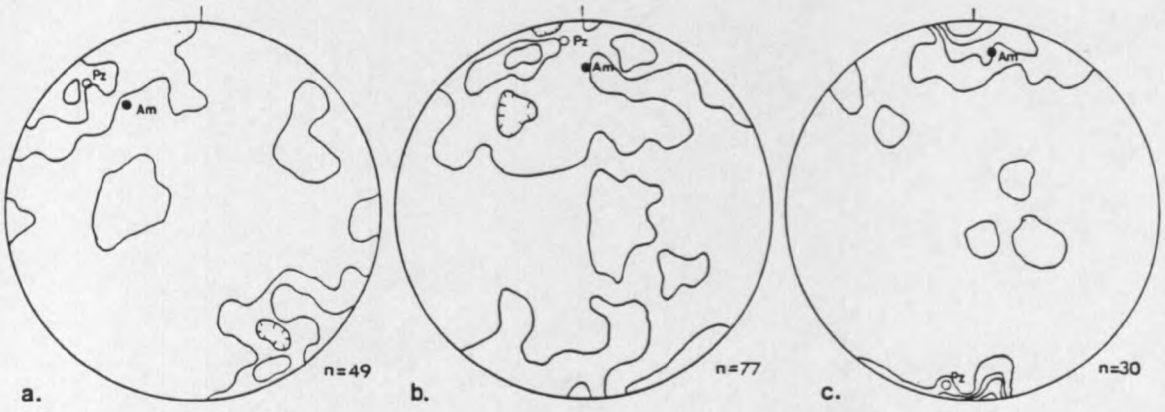

Figure 18. b kinematic directions of foliation-oblique mesoscopic faults from the a) Canyon Mountain b) western and c) central anticlines. Open circle is Paleozoic fold axis. Solid circle is basement fold axis. Contour intervals are 0, 5, 10, and 15 % per 1% area.

Seventy-seven foliation oblique faults from the western anticline were plotted to distinguish fault geometries and their kinematic role. The angle between fracture and foliation is shown in relation to the acute angle between the b kinematic axis and fracture-foliation intersection (Price, 1966)(Figure 19). Three categories of faults are distinguished by this plot. Contraction faults (group I) show primarily dip slip motion and make an angle between 30°-50° with

the foliation surface. Extension faults (group II), also dip-slip, form an angle of 70°-90° with the adjacent foliation surface. Group III faults are primarily strike-slip and form a high angle with the adjacent foliation surface. These faults serve specific kinematic roles in passive-slip folding and accommodating bending strain (tangential longitudinal strain), as discussed below.

Passive-slip. Contractional faults (group I)(Figure 19) form in regions where pre-Laramide foliation attitude was at a high angle to the shearing stress imposed by interfolial slip. As flexural-slip folding progressed, shear stress on foliation surfaces was relieved by interfolial slip and the maximum principle stress direction became foliation-parallel (Parker and Donath, 1964; Price, 1966).

Most contractional faults form a 35° to 45° angle with the adjacent foliation surface. Insight into deviation from the 30° value predicted by Mohr-Coulomb fracture theory is provided by triaxial compression tests performed on anisotropic rocks (Donath, 1964). These tests demonstrate that for anisotropy orientations of 45°-75° to the maximum principle stress, the resulting shear fracture occurs at 45° to the maximum principle stress. For orientations less than 45° to the maximum principle stress, the fracture follows the anisotropy. Therefore, in regions where interfolial slip was impeded by Archean folds, the resulting fault occurred most frequently at 45° with respect to the adjacent foliation surface. Where the foliation was oriented at an angle less than 45°, layer-parallel slip occurred.

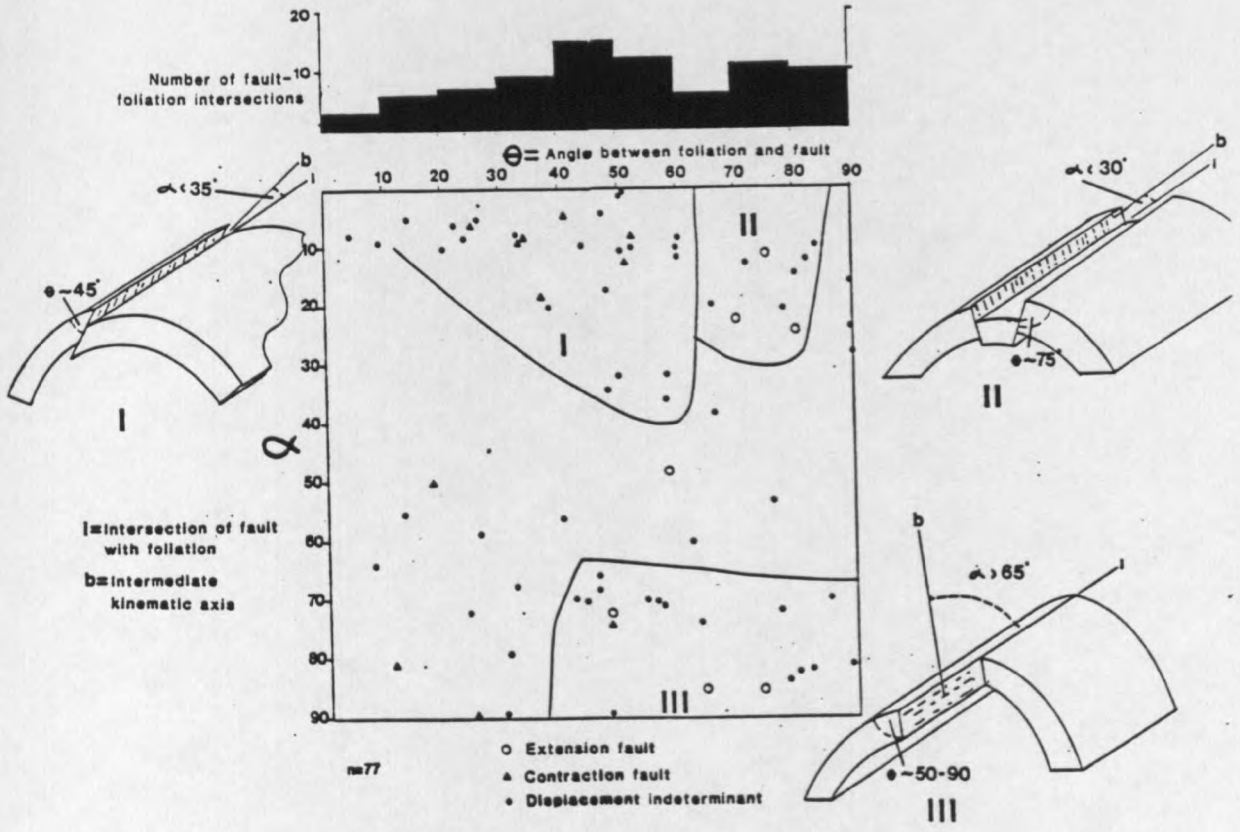

Figure 19. Faults plotted with b©i (angle between b kinematic axis and line of intersection, i, of foliation and fault surfaces) as ordinate; the angle between foliation and fault (θ) plotted as abscissa. Number of fault-foliation intersections is plotted at the top (after Price, 1966).

Passive-slip faults were recognized in the field by offset F1 and F2 fold hinges. Mesoscopic faults with offset of several centimeters shear limbs and hinges of small F2 folds (Figure 20). Larger F1 and F2 folds buttressed interfolial slip similar to the smaller folds, but the resulting shear surfaces are wide zones of cataclasis (Figure 21).

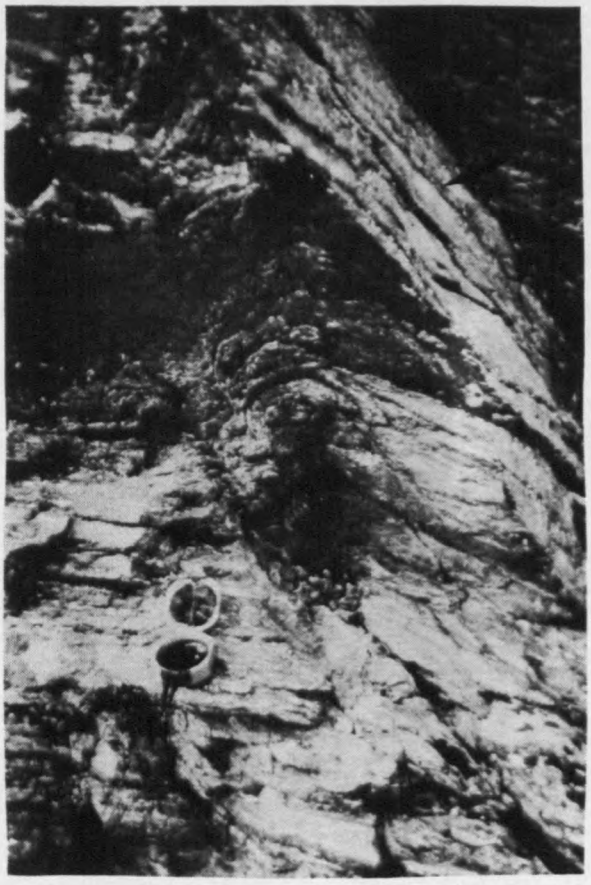

Figure 20. A sheared F2 fold on the east limb the western anticline, Bridger Range. View is looking north. The fold blocked layer-parallel shear and resulted in a passive-slip fault (designated by arrow) that offsets the backlimb. Fault forms a 45° angle with the adjacent foliation.

Figure 21. Cataclastic shear zone bounds meter-scale block of near vertical foliation on west limb of western anticline. View is looking north. Shear zone is parallel to underlying foliation. Flexing of foliation surfaces in the upper block indicates transport is towards the fold hinge (right). Shear zone is interpreted as a passive slip surface which offsets foliation disrupted by Archean folding. Foliation surfaces in the upper block have no kinematic role in the deformation and indicate macrogranular deformation. Relationship of this shear zone to the anticline is shown in figure 22.

Tangential Longitudinal Strain

Buckling of a nonstratified sheet will result in strains which have their principle axes oriented tangentially and perpendicular to the folded layer (Ramsay, 1967, p. 397). These strains are extensional on the outer surface of the layer and contractional on the inner surface.

Between the regions of contraction and extension lies a surface of zero tangential longitudinal strain known as the "finite neutral surface" (Ramsay, 1967, p. 398). A few of the contraction faults that were not associated with shortening in regions of Archean folding are interpreted as accommodating inner arc shortening. However, as will be explained in the next section, thick mechanical units tend to break into rigid body segments with no internal strain. Thus, there are comparatively few contraction faults related to inner arc shortening.

Normal faults (group II)(Figure 19) form in response to tangential longitudinal strain above the neutral surface. Normal faults occur most frequently along the hinge zone where outer arc strain is greatest. These faults are interpreted to be instrumental in the break up of the buckled layer into macrogranular blocks. Strike-slip faults (group III) bound macrogranular blocks where they accommodate shear, oblique to the axial plane.

Macrogranular Displacements

Macrogranular displacements are indicated where large, internally undeformed blocks have been passively rotated and translated along cataclastic shear zones (Figures 21, 22, and 23). Absence of internal deformation is seen in undisrupted, large wavelength, F1 and F2 folds within the blocks. In some cases, the wavelength of these folds controlled the thickness of the block (Figure 22). Abundance of leucocratic minerals and absence of discrete mica layers also contributed to the unstratified response. Extensional faults (group II) and fractures as well as shear faults (group III) bound these blocks.

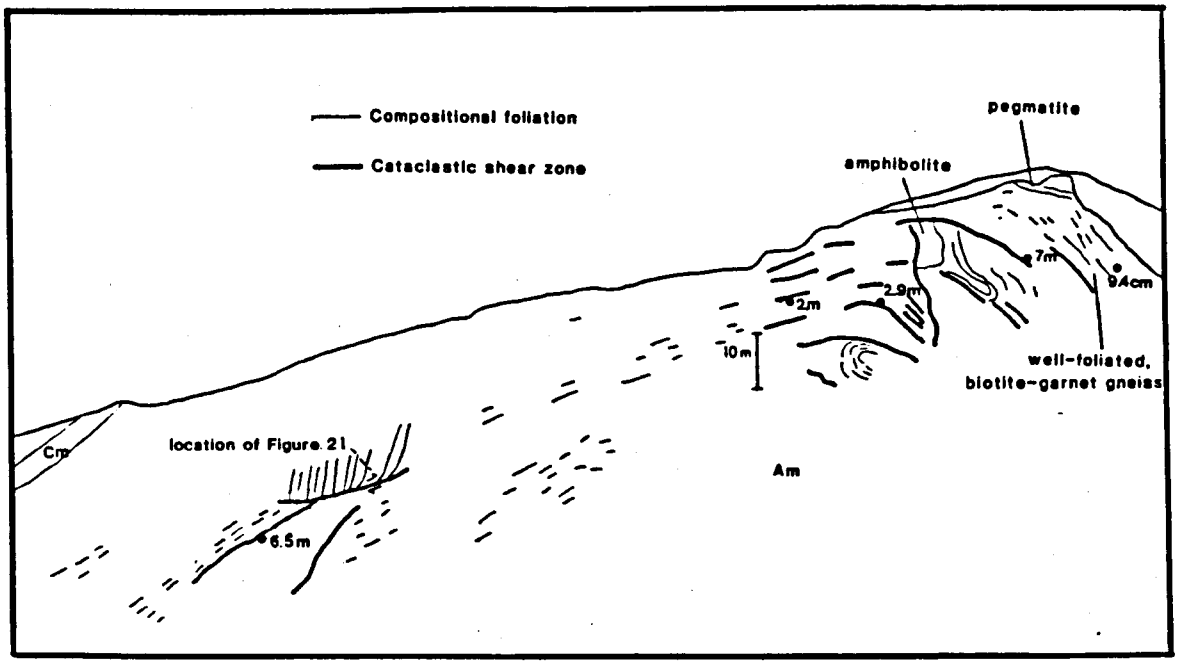

Figure 22. Line sketch based on photo mosaic of the western anticline. View is looking north. Line of drawing is A-A' in Figure 5. Right side of sketch is shown in Figure 7. Heavy lines are cataclastic shear zones. Thin lines are foliation surfaces. Note development of cataclastic shear zones in regions of Archean folding. Folds inhibit slip along foliation surfaces and result in large blocks which are internally undeformed (blocks indicated by arrows). Cataclastic shear zones are narrow (<5 centimeters) or absent in well foliated garnet-amphibolite gneisses and schists on east limb of fold. Numbers are slip estimates based on thicknesses and dip of mechanical foliation units.

These observations indicate that although the basement was foliated on a centimeter scale, in places the lithologic foliation played no mechanical role in the deformation. Apparently, break-up and extension of these mechanically thick units into macrogranular segments was preferred over coherent deformation with large amounts of tangential longitudinal strain.

Shear Strain Estimates

A variety of small-scale structures reflect the shear strain accommodated in large cataclastic shear zones. In several shear zones, a ductility contrast is present between cataclastically deformed material and rigid feldspar and amphibolite layers. Shear strain was accommodated in these layers by normal and contraction faults, brittle boudins, and brittle folds (Figure 24). Because the deformed layers were initially parallel to shear zone walls, there is no method available to compute the amount of strain from their deformation (Ramsay, 1980; 1983).

However, the strain accommodated by slip (s) along the outer surface of a folded layer of thickness (t) can be computed based on limb dip (α)(in radians) by the relationship:

$$s = t\alpha$$ (Ramsay, 1967, p. 393).

This relationship also explains the absence of thick cataclastic shear zones in well-foliated rocks. Where the basement is characterized by well-foliated biotite gneiss, such as on the east limb of the western anticline (Figure 22), slip surfaces occur at 10-20 centimeter intervals. Slip estimates based on the maximum observed limb dip of 60° show 9 centimeters of slip (Figure 22). Thus, rocks with closely spaced foliation surfaces underwent small amounts of slip spaced over a large number of slip surfaces. Biotite on these surfaces provided discrete layers of low cohesive strength which acted as slip surfaces during deformation.

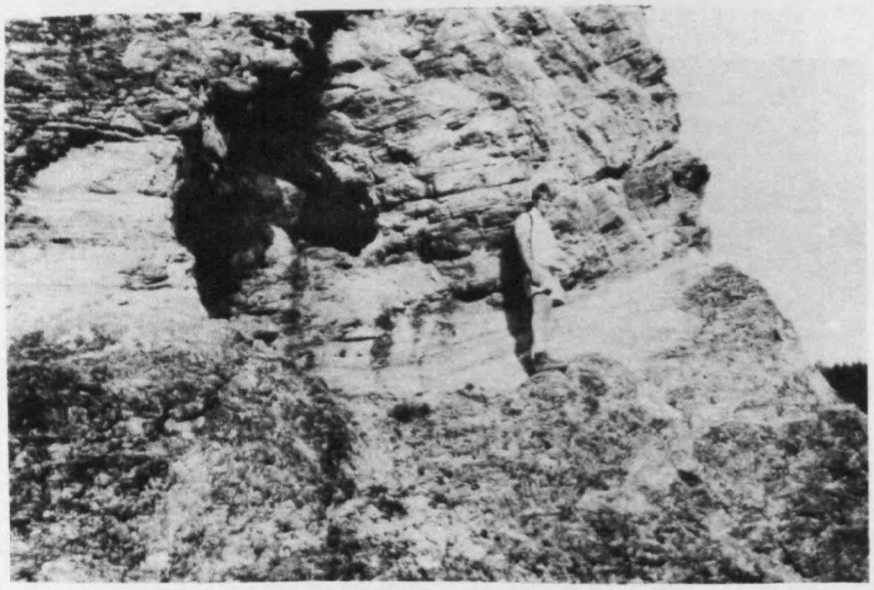

Figure 23. One meter thick cataclastic shear zone in the western anticline. View is looking east, into the axial plane of the western anticline. Shear zone is shown by arrow on the left side (west) side of Figure 7. Note man for scale.

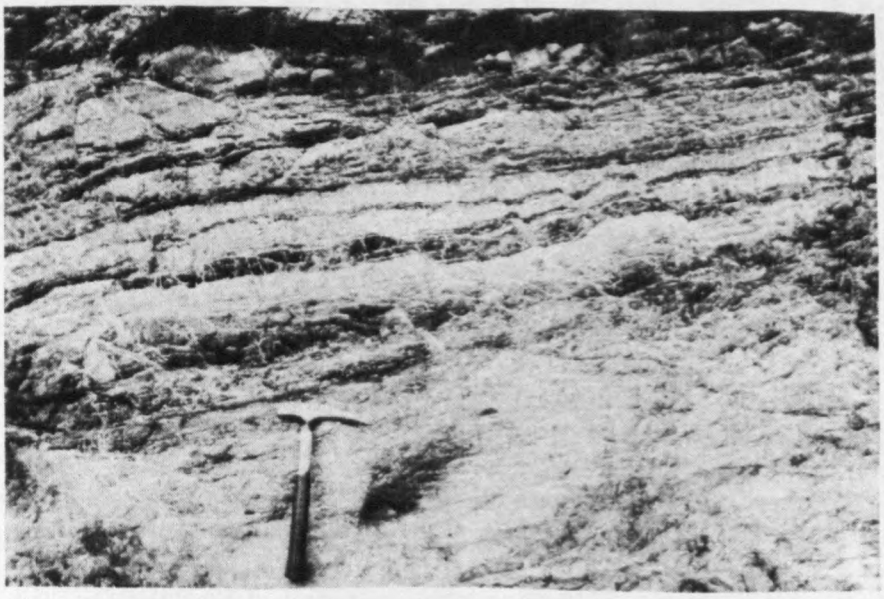

Figure 24. A brittle, amphibolite layer which accommodated extension due to simple shear by small-scale normal faulting. A contraction fault, on the left side, formed in response to shortening. Both fault sets are synthetic and indicate dextral slip along the shear zone. Zone is located on the west limb of the western anticline. View is looking north, parallel to the fold axis.

Zones of cataclasis, on the other hand, are indicative of large amounts of shear strain accompanying macrogranular movement of mechanically thick, unstratified units. Thicknesses of these units range from 5 - 12 meters (Figure 22). Slip calculations indicate up to 7 meters of slip has occurred along the boundaries of these blocks (Figure 22). The mechanics of deformation in these shear zones is presented in Chapter 4.

The kinematic elements of deformation for the flexural-slip "fold model" are summarized in an idealized Laramide anticline where the angle of discordance between foliation surfaces and the overlying strata is low (Figure 25). In Chapter 5, the relative amount of deformation accomplished by passive-slip is shown to increase in compositionally isotropic rocks.

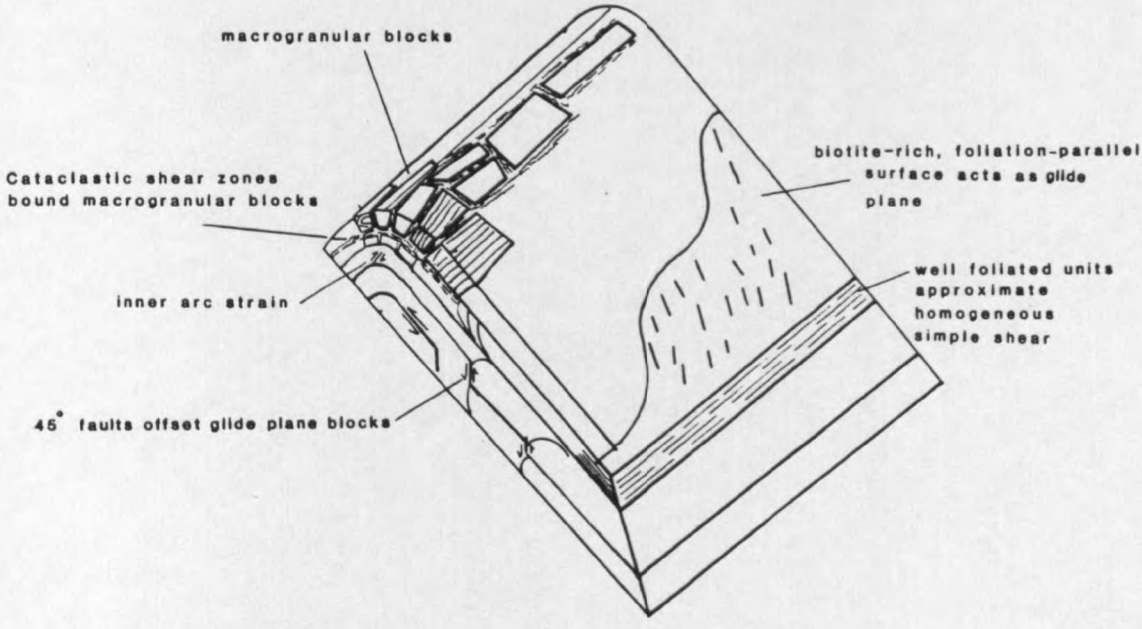

Figure 25. A model of basement deformation in regions with a low angle of discordance between the sedimentary cover and basement foliation surfaces.

LARAMIDE SHEAR ZONE DEFORMATION

Shear zones are loosely defined as narrow, sub-parallel zones characterized by large amounts of deformation (Ramsay, 1980). These zones represent discrete strain discontinuities that accommodated Laramide basement shortening. Mesoscopic and microscopic observations of shear zones reveal characteristics of brittle and brittle-ductile deformation in a near-surface (< 2km), sub-greenschist environment where hydrothermal played a critical role. Deformational mechanisms show a transition from mechanical fracturing to pressure solution with decreasing grain size. Retrograde metamorphism was deformation-enhanced.

Metamorphism

Pre-Laramide Mineral Assemblages

The pre-Laramide mineral assemblages chosen for detailed petrographic study are typical of almandine zone, amphibolite-facies metamorphism (Turner, 1968). Rocks indicative of sillmanite zone metamorphism have been identified in the northern Gallatin Range (May, 1986), although none were examined in this study. Quartzofeldspathic rocks of the central and western anticlines are characterized by the assemblage An_{30} + K-feldspar + biotite + quartz. At Canyon Mountain and the western anticlines, basic rocks are characterized by the assemblage: ferrohastingsite + An_{30} + quartz $\pm$ biotite $\pm$ garnet $\pm$ K-feldspar. In thin sections of rocks unaffected by Laramide

deformation, the pre-Laramide assemblages possess smooth, slightly curved grain boundaries and polygonal arcs around small scale F2 folds, indicating that mineral forming reactions were arrested close to equilibrium.

Laramide Mineral Phases: Occurrence

Epidote. Epidote occurs as a common reequilibration product of tectonically deformed plagioclase. Its presence in shear zones, characterized by alternating episodes of dilation and shearing, suggest it formed over a protracted period of deformation (Figure 26).

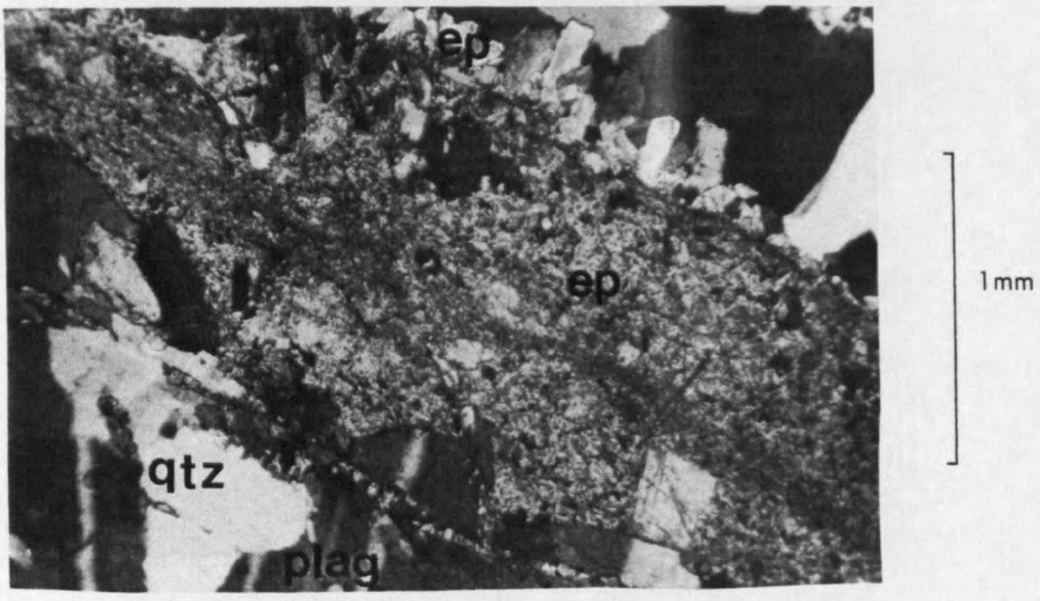

Figure 26. Cataclastically deformed epidote in shear zone center, and euhedral epidote along zone margin indicate a protracted period of epidote formation. Note preferred growth of epidote perpendicular to the zone wall. Shear zone from which this sample was obtained offsets an F2 fold hinge in the central anticline.

Chlorite. Chlorite is the most abundant Laramide phase and replaces hornblende, garnet and plagioclase. Only minor amounts of chlorite are associated with reequilibration of plagioclase, where it is found with epidote and quartz. The formation of chlorite from biotite and hornblende occurred extensively along foliation-parallel shear zones.

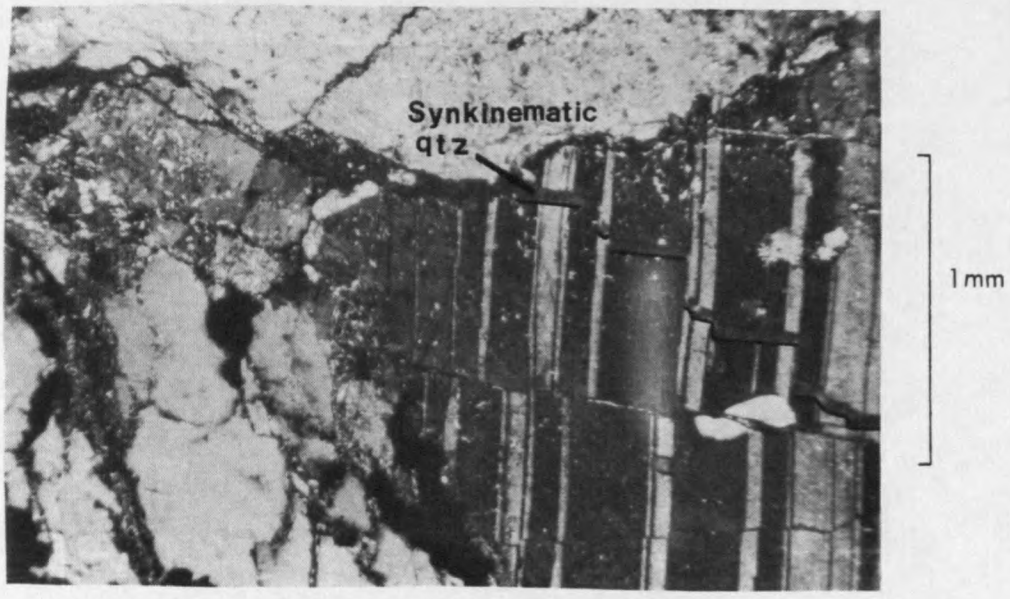

Figure 27. Synkinematic quartz precipitation records slip along albite twins in a plagioclase grain. Horizontal shearing of plagioclase grain post dates slip along twins. Thin section is from the margin of a 1 meter wide cataclastic shear zone in the western anticline.

Quartz. Quartz occurs as vein filling material and as anhedral blebs and stringers related to reequilibration of plagioclase, biotite, and hornblende. Syntectonic quartz vein filling occurs in numerous microfractures which predate and postdate zones of cataclasis (Figure 27).

Sericite. Sericite was found as a secondary alteration product of plagioclase and is conspicuously absent on most K-feldspar grains. Much of the sericite appears as disseminated flecks encased in plagioclase grains, or as stringers forming preferentially along albite twins.

Actinolite. Actinolite occurs as minute, undeformed, elongate, randomly oriented crystals that post-date deformation. Its occurrence is restricted to shear zones that truncate and offset veins of euhedral epidote.

Hematite. Hematite was identified in the field on slickensided slip surfaces. In thin section, hematite occurs as opaque blebs along microcracks and microfaults. It is often associated with chloritized biotite.

Calcite Calcite occurs as euhedral vein filling which cross-cuts all other microfaults and veins.

Physical Conditions of Deformation

Although epidote, actinolite, and chlorite are present, the greenschist assemblage (albite + actinolite + epidote + chlorite) was not identified (Turner, 1968). This mineralogy indicates conditions of deformation were sub-greenschist facies. However, presence of epidote suggests fluid temperatures were considerably hotter than ambient conditions. Ambient conditions were characterized by a maximum lithostatic pressure of 670 bars (based on an average geobaric gradient of 0.3 kilobars/ kilometer and 2 kilometers of Phanerozoic

overburden) and a rock temperature of 80°centigrade (based on a high geothermal gradient of 40°centigrade/kilometer)(Best, 1982). Investigations into the lower stability limit of epidote, based on natural occurrences, indicates the minimum temperature of formation is approximately 200°C at 670 bars (Seki, 1972). This temperature is based on conditions of formation in iron-rich basalts that possess oxidizing conditions (Seki, 1972). A decrease in iron or oxygen fugacity would only increase the minimum temperature of epidote stability (Liou, 1972).

Mechanisms of Shear Zone Deformation

On a microscopic scale, shear zones show characteristics of brittle and brittle-ductile deformation. In brittle deformation, rupture is a spontaneous event marked by a rapid decrease in stress that accompanies fracturing (Paterson, 1978). In the rock record, brittle processes are marked by unstable fractures that cut across grain boundaries (Mitra, 1984). These fractures shear off polycrystalline fragments of wall rock. Internally, these aggregates show no sign of ductile deformation, indicating that stresses were relieved instantaneously (Mitra, 1984).

The heterogeneous mineralogy of the quartzofeldspathic basement rocks resulted in brittle and ductile processes operating concurrently during some stages of deformation. These brittle-ductile zones are characterized by stable fractures that end at grain boundaries (Paterson, 1979; Mitra, 1984). Strain accommodation in the surrounding grains occurs by ductile processes of either cataclastic

flow, dislocation gliding, or diffusion (Mitra, 1984).

In Chapter 3 (Figure 22), shear zone width was shown to increase with increasing strain. Thus, an individual shear zone records progressive deformation from the outer to inner zone (Mitra, 1978). This process involves work hardening of the fracture zone such that continued shearing incorporates fresh wall rock (Mitra, 1978). The following discussion records the sequence of deformation across a narrow zone of intense deformation based on mineralogical and textural criteria. Mesoscopically, a single shear zone is comprised of an intricate, anastamosing system of these zones.

Stage I - Unstable Fracturing

The initial stages of deformation are marked by predominantly brittle processes along shear zone walls. Unstable fracturing was characteristic and is seen in numerous fractures that cut across grain boundaries (Patterson, 1978). Lenticular rock fragments, parallel to the zone margin, suggest that sliding occurred parallel to the zone wall. Further fracturing and wear due to frictional sliding is inferred by a progressive decrease in grain size with distance from the zone margin (Figure 28; zone 1). As the percentage of matrix increases (Figure 29; zones 1-2), a transition from unstable to stable fracturing occurs.

Stage II - Cataclastic flow.

The inner zone is characterized by distinct zones of microbreccia and cataclasite, separated by narrow zones of mylonite. Grains in the microbreccias and cataclasites (Higgins, 1971) are

subangular and appear to float in the matrix (Figure 30). Angular porphyroclasts provide evidence that the majority of strain in this zone was accommodated by cataclastic flow along glide bands in the matrix (Mitra, 1984). Thus, frictional wear was less important at this stage.

Plagioclase grains show intense sercitic and epidotic alteration and provide evidence for increased permeability and metasomatism compared to the zone margin. This chemical alteration may have lowered the structural integrity of the grains and enhanced further deformation (White, 1975).

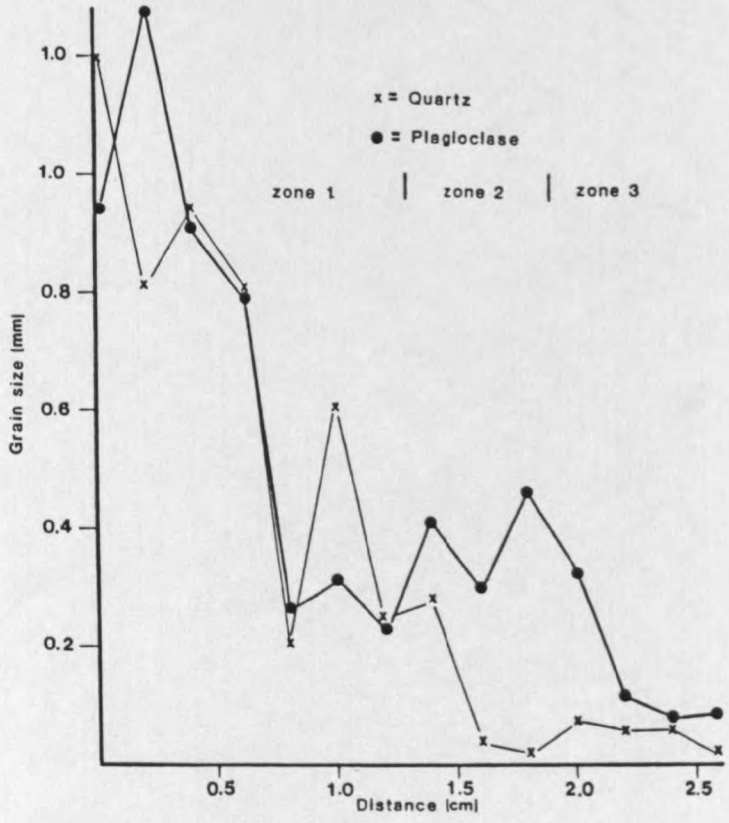

Figure 28. A plot of grain size versus distance shows a decrease in grain size with increased distance from the shear zone margin. Zones 1, 2, and 3 correspond to deformational stages discussed in the text (after Mitra, 1984).

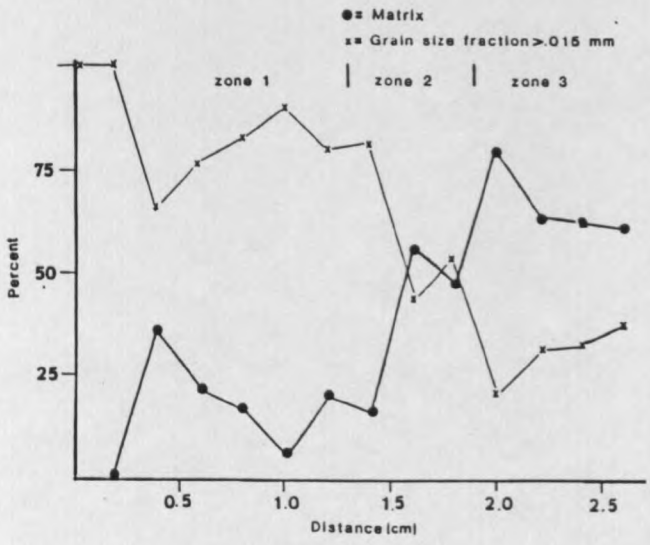

Figure 29. A plot of percent matrix versus distance from the shear zone margin shows an increase in matrix with increased distance from the shear zone margin (after Mitra, 1984).

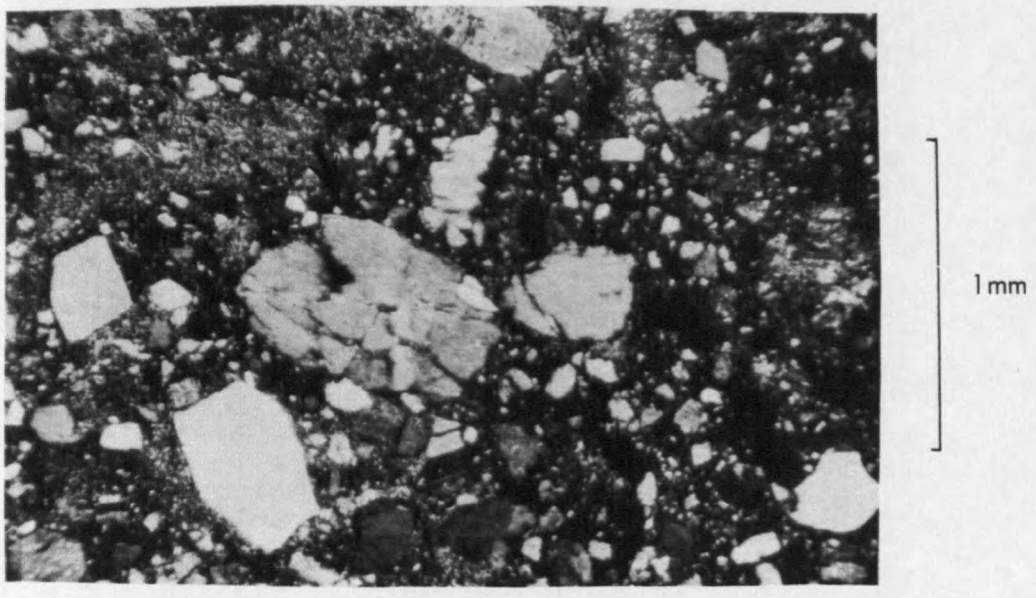

Figure 30. Zone 2 is characterized by a microbreccia. Angular fragments indicate the matrix yielded by cataclastic flow. Note stable fracturing of grain (arrow) in center of photomicrograph .

With decreasing grain size, an increase in applied stress was necessary for further fracturing. This relationship is known in the metallurgical literature as the Hall-Petch relationship and was first applied to geological situations by Mitra (1978):

$$\sigma_f = \sigma_o + K/d^{(-1/2)} \qquad \text{(Mitra, 1978).}$$

Where σ_f is the applied stress, σ_o is the stress from friction due to dislocation pile ups, K is a material constant and d is grain size. The Hall-Petch relationship indicates that for a constant applied stress, continued grain size reduction results in strain hardening within the fault zone (Mitra, 1978, 1984). Eventually, a minimum grain size will be reached that is inversely proportional to the square of the applied stress. A transition then occurs where further grain deformation is inferred to occur by chemical processes (Mitra, 1984).

Stage III - Pressure Solution and Dislocation Processes

The inner-zone mylonite has a well-developed, secondary foliation characterized by flattened quartz grains in an anstamosing matrix of clay and hematite (Figure 31). This zone is deficient in more mobile constituents such as quartz, but shows an increase in insoluble residues of clay and hematite. The relative abundances of these minerals indicates deformation in this zone occurred, to some degree, by pressure solution (Ramsay, 1980; Elliott, 1973). Absence of overgrowths suggests the dissolved material moved into regions of low pressure in neighboring cracks and is now preserved as syntectonic vein

filling (Figure 27). Larger, flattened quartz grains show low-angle subgrains oriented parallel to the shear zone walls. Thus, some internal strain was also accommodated by dislocation processes.

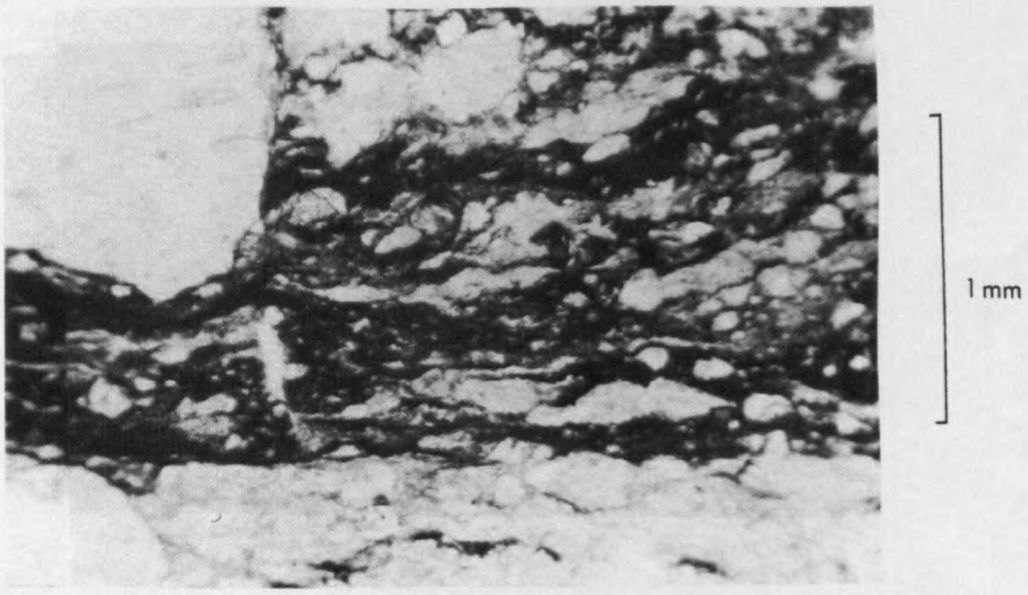

Figure 31. The zone 3 mylonite is characterized by anastamosing clay and iron oxide surrounding microlithons of flattened quartz. Photo taken in plane light.

The decrease in grain size during stages 1 and 2 (Figure 30) deformation, accompanied by an increase in diffusional processes in zone 3, is in accordance with the diffusional flow law (Elliott, 1973). As fault development progressed to zone 3 deformation, a high percent of saturated matrix (Figure 29) is inferred to have induced a transition from frictional sliding along microcracks to diffusion processes. Similar transitions have been noted in crystalline basement rocks in the internal regions of thrust belts (Mitra, 1978) and in limestone thrust sheets in the external part of the foreland (Wojtal and Mitra, 1986).

Other Studies of Laramide Shear Zone Deformation and Metamorphism

A very small body of knowledge exists concerning Laramide overprinting of Precambrian assemblages. Bruhn and Beck (1983) noted a greenschist overprint in shear zones associated with Sevier-style thrusting of quartz-monzonite gneiss of the Precambrian Farmington Canyon Complex along the Ogden thrust. The retrograde assemblage identified was epidote, chlorite, stilpnomelane, and sericite. Mineral textures of these rocks are similar to those identified in this study and include pulverized and sheared epidote and streaked out phyllosilicates along fault surfaces.

Hoppin (1970) noted that epidotization and chloritization accompanied deformation in Laramide shear zones which bound the northwest flank of the Bighorn Range. The protolith in this region was a biotite-quartz-oligioclase gneiss. Intensity of alteration increased with proximity to the shear zones.

In the Wind River Range, Wyoming , Mitra and Frost (1983) proposed deformation in Laramide shear zones occurred under zeolite conditions (1 kilobar; 150° centigrade), with only small amounts of fluid present in the system. Their proposed conditions of deformation were based on the growth of phengitic mica along shear zones in the Flathead Sandstone.

Mitra (1984) concluded that deformation along the White Rock thrust, an imbricate splay of the Wind River thrust, occurred at 4 kilobars and 250°centigrade based on palinspastic restoration. Deformational mechanisms show a transition from brittle to brittle-

ductile processes and an increase in diffusional processes with time. The textures of these zones are similar to those identified in this study. However, in the White Rock thrust zone, only minor amounts of fluid were present and the transition from brittle to brittle-ductile deformation is attributed to large strains (Mitra, 1984). Significant retrograde mineralization in the shear zones of the Bridger and Gallatin Ranges indicate the transition from brittle to brittle-ductile processes occurred in response to fluid influx. Although the pressure and temperature conditions are similar to those identified in Laramide shear zones of southwest Montana, absence of fluids in the Wind River Range allowed only a minimum of mineral reequilibration. Thus, conditions of deformation noted in this study appear more closely related to those along the Ogden thrust and Bighorn Range.

MODELS OF FORELAND UPLIFTS

Drape fold (Stearns, 1978), fold-thrust (Berg, 1962; Brown, 1983), and thrust-fold models (Stone, 1984; Erslev, 1986) have emerged as interpretive models for the geometry and origin of foreland uplifts. Interpretations based on detailed field work in this and other studies (Erslev, 1986) indicate the thrust-fold model has applications to non-fold structures such as Squaw Creek fault.

In regions where the sedimentary cover is folded and the basement-sedimentary nonconformity is available for direct observation, investigators have recognized a mobile basement (fold model). The mobile basement is compatible with the fold-thrust model (Berg, 1962). Canyon Mountain anticline and the Bridger Range are shown to be specific examples of the fold-thrust model based on geometric and kinematic relations. This and other field studies indicate folding of the basement is accomplished by a spectrum of mechanisms ranging from flexural-slip to passive-slip to cataclastic-flow.

Drape Fold Concept

Drape folds or force folds are defined as folds where the geometry of the strata is imposed by a lower forcing member (Stearns, 1978). In its classic form, the sedimentary strata are passively draped over steps defined by differential uplift of basement blocks. The basement behaves rigidly and undergoes primarily vertical uplift with some minor rotation of blocks (Stearns, 1978; Prucha and others, 1965).

Critics of the drape fold concept point to a disregard for a geometrically feasible basement configuration (Stone, 1984). Restoration of basement block uplifts to their pre-Laramide position leads to major gaps (for cross sections with vertical faults) or overlaps (for cross sections with fleur-de-lis faults). Furthermore, the stratal length which bounds the hanging wall cutoffs must be transferred along detachments between the sedimentary strata and basement blocks. Several researchers have noted that major basement detachments of this type do not exist (Hodgson, 1965; Blackstone, 1980; Stone, 1984; Schmidt and Garihan, 1983). In spite of these deficiencies, the drape-fold concept was popular among some geologists for over a decade.

COCORP seismic surveys largely dispelled the drape-fold model. Deep crustal, seismic reflection profiling show faults which maintain moderate dips down to the brittle-ductile transition, indicating the uplifts form in response to horizontal compression (Brewer and others, 1981; Brewer and others, 1983). Furthermore, oil and gas drilling has penetrated through basement overhangs into overturned Phanerozoic rocks as predicted by the fold-thrust model or thrust-fold model (Gries, 1983).

Fold-Thrust Model

The fold-thrust model is characterized by active folding of the basement and overlying sedimentary strata (Berg, 1962). The deformational sequence begins with development of an asymmetric, basement-cored anticline with a minor forelimb fault in the sedimentary

strata. Progressive folding results in faulting of the synclinal hinge, followed by rotation and overturning of the forelimb (Berg, 1962). Some thinning may occur on this limb from shearing along the fault zone. The result is a classic, "mountain front" overhang where basement rocks lie over younger sediments (Brown, 1983). Dynamically, the model is compatible with a region undergoing horizontal compression. Earthquake focal studies from basement-involved regions in the Andes (a modern analogue to Laramide-style deformation) indicate a region undergoing horizontal compression and corroborate the fold-thrust model (Jordan and others, 1983). Field evidence from Canyon Mountain anticline and the Bridger Range indicate these structures are compatible with the fold-thrust model.

Canyon Mountain Anticline

Schmidt and Garihan (1983) suggested a kinematic model for Canyon Mountain anticline that invokes east-west shortening along a preexisting normal fault. However, shortening directions, determined from mesoscopic fault data using the method of Allmendinger (1986), indicate northeast-southwest shortening in the core of Canyon Mountain anticline (Figure 32a). Slickenside lineations, measured along mesoscopic fault surfaces parallel to Suce Creek fault, show south-southwest transport and predominantly dip-slip movement (Figure 32b). This motion is not compatible with east-west shortening on a preexisting normal fault, where a large component of sinistral slip is expected (Schmidt and Garihan, 1985). However, it is compatible with northeast-southwest shortening. The coaxial shortening directions of Canyon Mountain anticline and Suce Creek fault suggest thrusting

accompanied basement folding.

A series of interbasement faults parallel Suce Creek thrust and indicate that some shortening was accommodated by axial-planar faulting in the core of the anticline. These faults occur as narrow (10 cm), cataclastic shear zones and, in places, bring up chloritized horses of amphibolite. In the center of the anticline, at a structurally deeper level, they occur as foliation-parallel shear zones. Where these faults intersect shear surfaces related to basement folding, they offset them, suggesting basement folding preceded faulting.

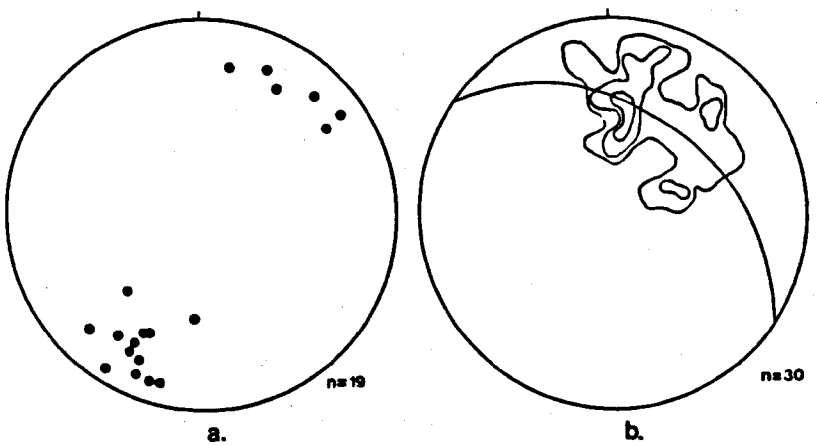

Figure 32. Shortening and transport direction are perpendicular to the fold axis at Canyon Mountain anticline. Equal area, lower hemisphere, stereographic projections. a) shortening directions based on mesoscopic faults and b) transport direction based on slickenside lineations measured along Suce Creek fault. Contour interval is 0, 5, 10, and 15 % per 1 % area.

These kinematic elements reveal the following movement history. Northeast-southwest shortening resulted in flexural-slip folding of subhorizontal foliation surfaces. With continued folding, the anticline became asymmetric, verging to the southwest. When the fold approached an interlimb angle of 100° (determined from the curved upper basement surface which can be continuously traced), shortening was

accommodated by axial planar sliding. Suce Creek thrust formed along Cambrian shales in response to crowding in the footwall syncline and cut down-section, possibly becoming foliation parallel at depth.

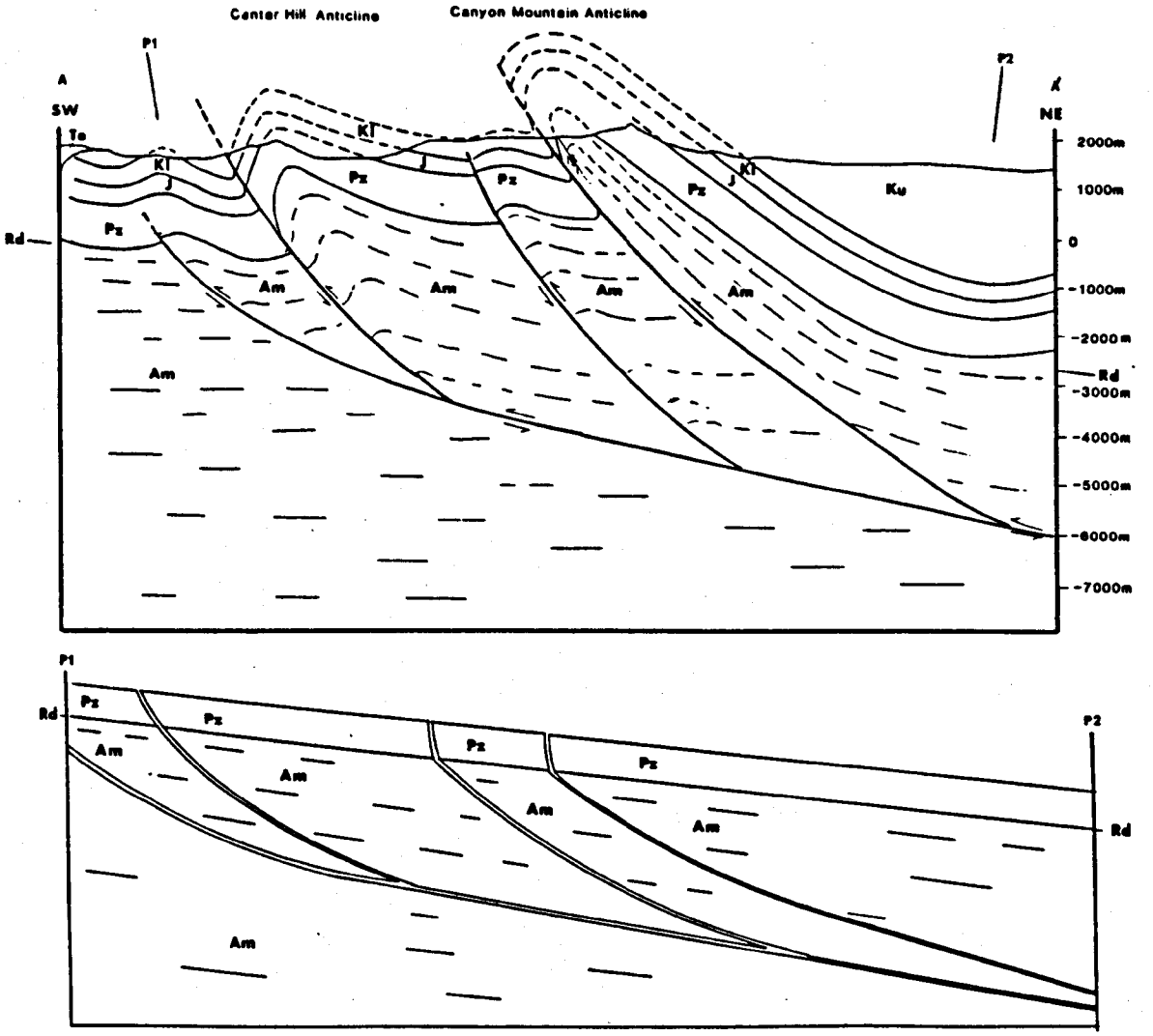

Figure 33. Cross section through Canyon Mountain anticline. Line of section is shown in Figure 2. P1 and P2 are pin points from Center Hill anticline and Fleshman Creek syncline respectively (Figure 2). Rd is regional dip that top of basement line length is restored to. Ku - Upper Cretaceous; K1 - Lower Cretaceous; J - Jurassic; Pz - Paleozoic; Am - Archean metamorphic rocks.

A cross section through Canyon Mountain anticline was constructed by modeling the basement as blocks which are capable of undergoing foliation-parallel shear (Figure 33). In addition to the geometry of the Phanerozoic sediments, the cross section is constrained by: 1) flexural slip folding of basement rocks, 2) foliation-parallel faults and, 3) subhorizontal pre-Laramide foliation attitude. The basement is restorable in line length and area along a regional dip of 7° (Figure 36, Rd). The regional dip may reflect uplift due to post-Laramide volcanism or rotation along a master fault.

Bridger Range

Seismic profiles across the southern Bridger Range show west-dipping basement faults subparallel to the axial plane of the Laramide Bridger Range anticline (Lageson and Zim, 1985). These faults are believed to be analogous to the foliation-parallel, cataclastic shear zones found at Canyon Mountain. An east-west shortening direction for development of the Bridger Range is inferred from mesoscopic fault strain data from the western anticline (Figure 34). A shortening direction perpendicular to the range trend, axial planar thrusts, and folded basement of the western and central anticlines are all characteristics that are compatible with the fold-thrust model (Berg, 1962; Brown, 1983) and support its application to the Bridger Range anticline as proposed by Lageson and Zim (1985).

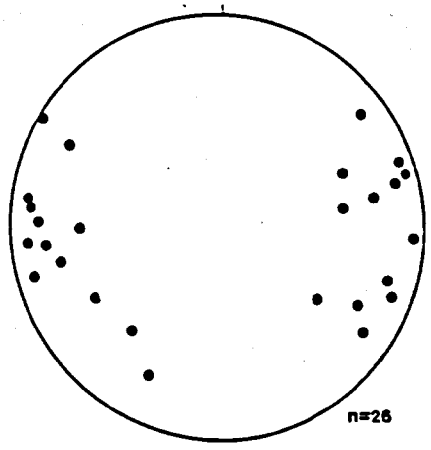

Figure 34. Shortening directions determined from mesoscopic faults in the western anticline, Bridger Range.

Thrust-Fold Model

Recent workers have attempted to reconcile the rigid basement rheology used by Stearns (1978) in a geometrically feasible manner that is dynamically compatible with horizontal compression (Spang and others, 1985; Erslev, 1985, 1986; Stone, 1984). Erslev (1985, 1986) suggested that the variation in stratal tilt between footwall and hanging wall blocks, as well as field observations of curved fault planes, justified a listric geometry for basement faults. Balanced cross sections (Dahlstrom, 1968) could be constructed by moving the basement blocks along an axis of rotation into their pre-Laramide orientation with a minimum of internal deformation. The restored basement would show no overlaps or gaps and have a flat, upper surface.

Kinematically, the overlying strata are force-folded around the hanging wall tip and cutoff to produce an anticline (Erslev, 1986). The extra strata length along the hanging wall cutoff is brought in by

a basement-sedimentary contact detachment (Robbins and Erslev, 1986). Synclinal folding on the footwall is accomplished by break off and rotation of the hanging wall tip to form a basement wedge (Erslev, 1986).

Stone (1984) originally coined this sequence of development the thrust-fold model. Its original form is based on a sequence of development inferred for the Pryor Mountains by Blackstone (1940). Stone's (1984) version differs from Erslev (1986) in that the synclinal folding is accomplished by imbrication of the footwall.

The thrust-fold model described by Erslev (1986) and Stone (1984) suffer the same shortcomings as the drape fold model by necessitating an upper-basement surface detachment. An application of this model to Canyon Mountain anticline by Robbins and Erslev (1986) invokes rigid basement blocks that are rotated along semicircular faults (Robbins and Erslev, 1986). A significant Cambrian-basement detachment allowed forced folding of the sedimentary strata. Field observations indicate that the basement is folded along foliation surfaces and that no major detachment is present. In order for a cross section to be correct, it must not only be geometrically restorable but must also honor all field relations (Elliott, 1983). Therefore, application of the thrust-fold model to Canyon Mountain anticline is not justified by this study.

However, by discarding the force-fold part of the thrust-fold model, it may be applied where field observations indicate a planar, basement surface (e.g. Forellen fault, Teton Range, Erslev, 1986). Application of the modified thrust-fold model to Squaw Creek fault is justified by the presence of a planar upper basement surface.

Kinematics of Non-Fold Model - Squaw Creek Fault

Squaw Creek fault was interpreted as a preexisting, normal fault that formed initially in response to rifting of the Belt basin (Schmidt and Garihan, 1983). Later, during east-west Laramide shortening, the fault underwent left-lateral, reverse slip. Schmidt and Garihan (1983) correlated this slip with other northwest-trending faults in the Montana foreland (e.g. Hinch Creek, Mammoth, and Bismark faults). In these faults, displacement differences between the Flathead Sandstone and marker units in the basement indicate that normal faulting occurred prior to Flathead deposition. Absence of distinctive marker units at Squaw Creek precludes conclusive evidence for reactivation of a preexisting normal fault. However, slickenside lineations, measured during this investigation, indicate a significant component of left-lateral slip (Figure 35). This movement is compatible with east-west shortening on a high-angle northwest-trending, reverse fault, and confirms the earlier observations of Schmidt and Garihan (1983).

A cross section was constructed using the method of Erslev (1986) (Figure 36). The cross section is constrained by: 1) a surface fault dip of 80°, 2) minimum stratigraphic displacement of 1273 meters, 3) planar basement surface indicated by the imbricate slice, 4) a hanging wall dip of 20°, and 5) a footwall dip of 10°. These data were used to calculate an axis of rotation which was used to graphically determine fault curvature (Erslev, 1986). The region where the fault flattens is inferred to be a zone of cataclastic deformation (Erslev,

1986). Rotation of footwall strata occurred through footwall imbrication and minor detachments in the Paleozoic shales. Disharmonic folding in the Cambrian Meagher Limestone above the planar Flathead-basement contact was identified in the field and justifies this geometry. However, no major detachments are involved, and hanging wall strata are truncated by Squaw Creek fault rather than force folded. This cross section (Figure 36) was constructed perpendicular to the fault trend. Because material was moving into and out of the plane of the cross section, the plane strain assumption may not be valid (Elliott, 1983).

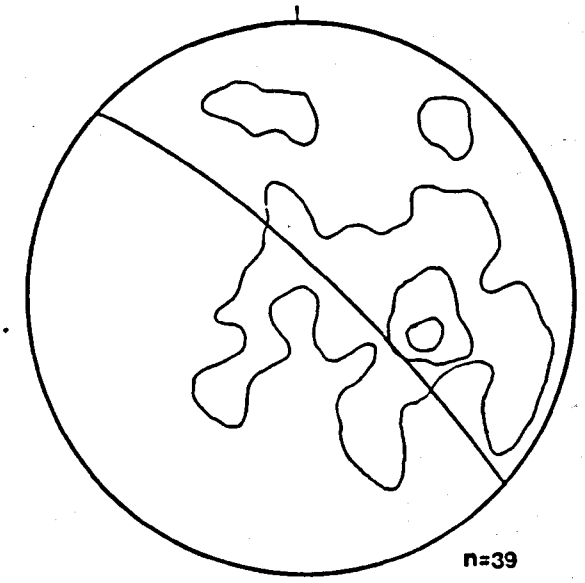

a.

Figure 35. Slickenside lineations measured along Squaw Creek fault. Great circle shows fault orientation. Contour interval is 0, 5, and 10 % per 1 % area.

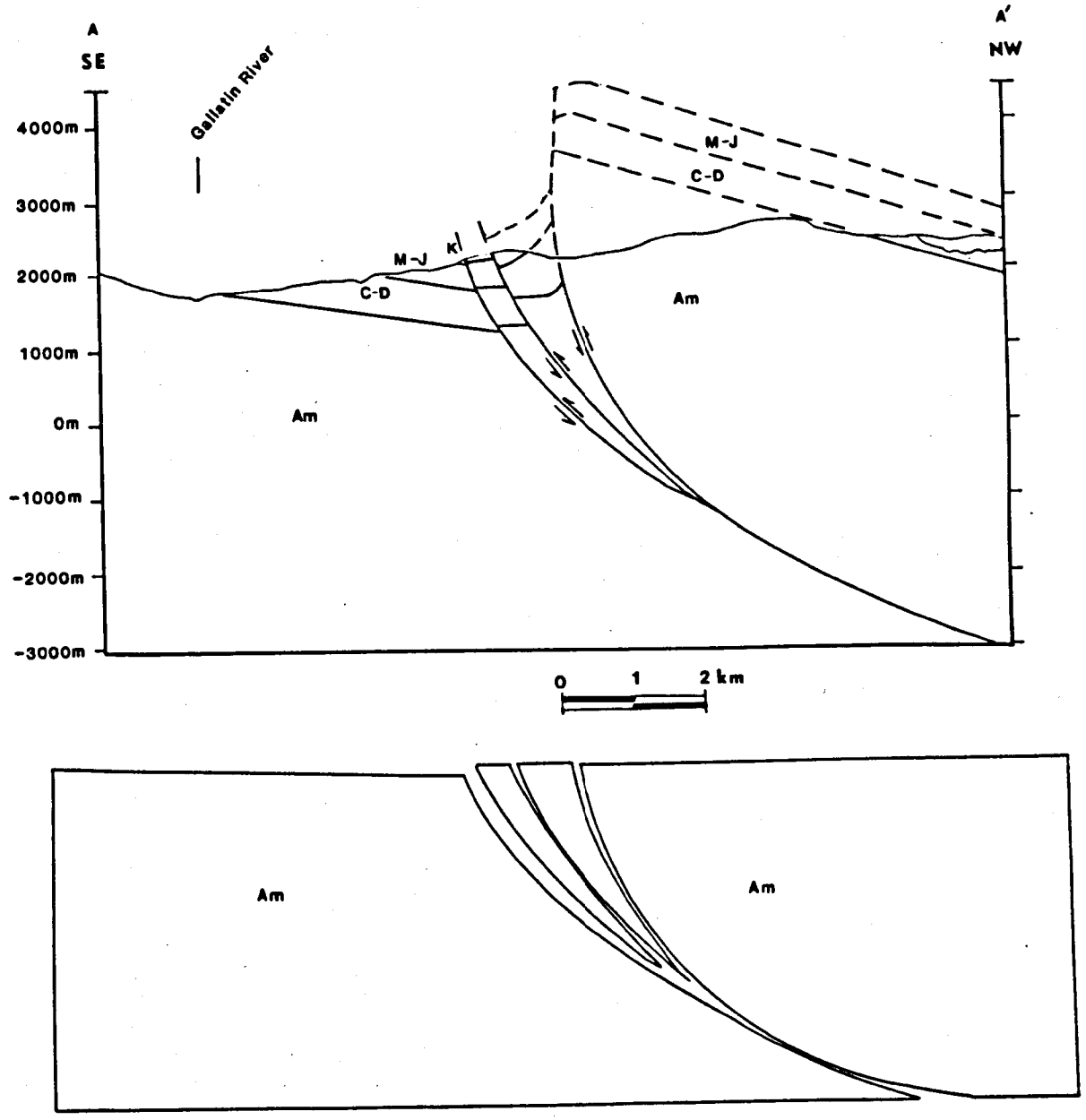

Figure 36. Balanced cross section through Squaw Creek which honors the planar upper basement surface observed in the field. Lower diagram shows restored basement which conserves area. The line of section is shown in Figure 14.

Two distinct styles of deformation along Squaw Creek fault are reflected in the strike-slip component. In the Timber Butte domain, Squaw Creek fault is foliation parallel. Apparently, Proterozoic extension exploited zones of low cohesive strength parallel to the steep-dipping, northwest-trending foliation. Shear strain, related to Laramide shortening, was also localized along this discrete discontinuity. Slickensided fault surfaces are conspicuously absent in the hanging wall and support a rigid basement model in which shortening is accommodated along a discrete fault zone (Erslev, 1986). In the footwall, however, two northwest-trending folds in Mississippian strata are truncated obliquely by the fault (Figure 14c).

The variable response of the basement and Paleozoic strata is explained by a detachment in the Paleozoic shales. The Cambrian shales acted as a zone of detachment and distributed left-lateral, reverse-slip movement of the basement into a wide zone of left-lateral, simple shear in the upper Paleozoic rocks. This imposed shear strain resulted in development of two, en echelon folds in Mississippian strata. Extension occurred parallel to the fold axis and was manifested as a series of mesoscopic normal faults. A minor detachment, such as the one proposed for this model, is exposed in the Cambrian Wolsey Shale in the central anticline.

A different basement response occurred in the northwest segment. In this domain, the foliation has a northeast strike and steep dip. Mesoscopic, northeast-trending, basement faults parallel foliation and show predominantly strike-slip motion (Figure 37). These faults occur primarily in the exposed basement of the imbricate wedge and

indicate a model where strain was accommodated by synthetic shears controlled by foliation, analogous to Riedel shear faults (Wilson, 1982). The northeast-trending basement faults may be mesoscopic reflections of the northeast-trending, map-scale faults in the footwall (Figure 14). These faults also show synthetic, left-lateral shear similar to the model of Riedel (1929).

In summary, the rigid, hanging wall basement rocks, planar, upper basement surface, and absence of major detachments indicate deformation at Squaw Creek occurred by rigid body rotation along listric faults. Slickenside lineations, folding of Mississippian strata, and Riedel shears provide evidence that significant translations occurred parallel to the fault plane. The basement response at Squaw Creek is most closely modeled by the thrust-fold model (Stone, 1984). However, the absence of any major basement-sedimentary detachment invalidates force-fold deformation for the overlying sediments.

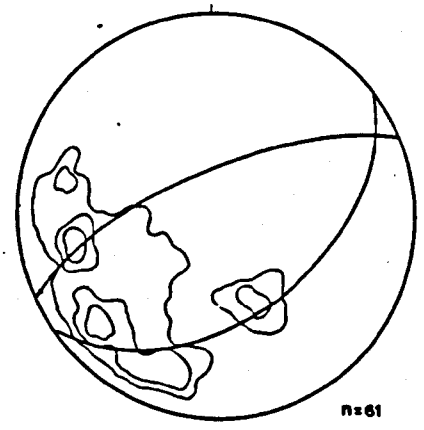

Figure 37. Slickenside lineations measured on northeast trending faults in imbricate slice of Squaw Creek fault. Great circles show mean fault orientations. Contour interval is 0, 5 and 10% per 1% area.

Spectrum of Deformation

Detailed field investigations of basement deformation in areas where the overlying sedimentary cover is folded, document active basement folding (Figure 38)(Table 1). The basement folds by a spectrum of mechanisms that include flexural slip, passive slip, and cataclastic flow as mechanical end members.

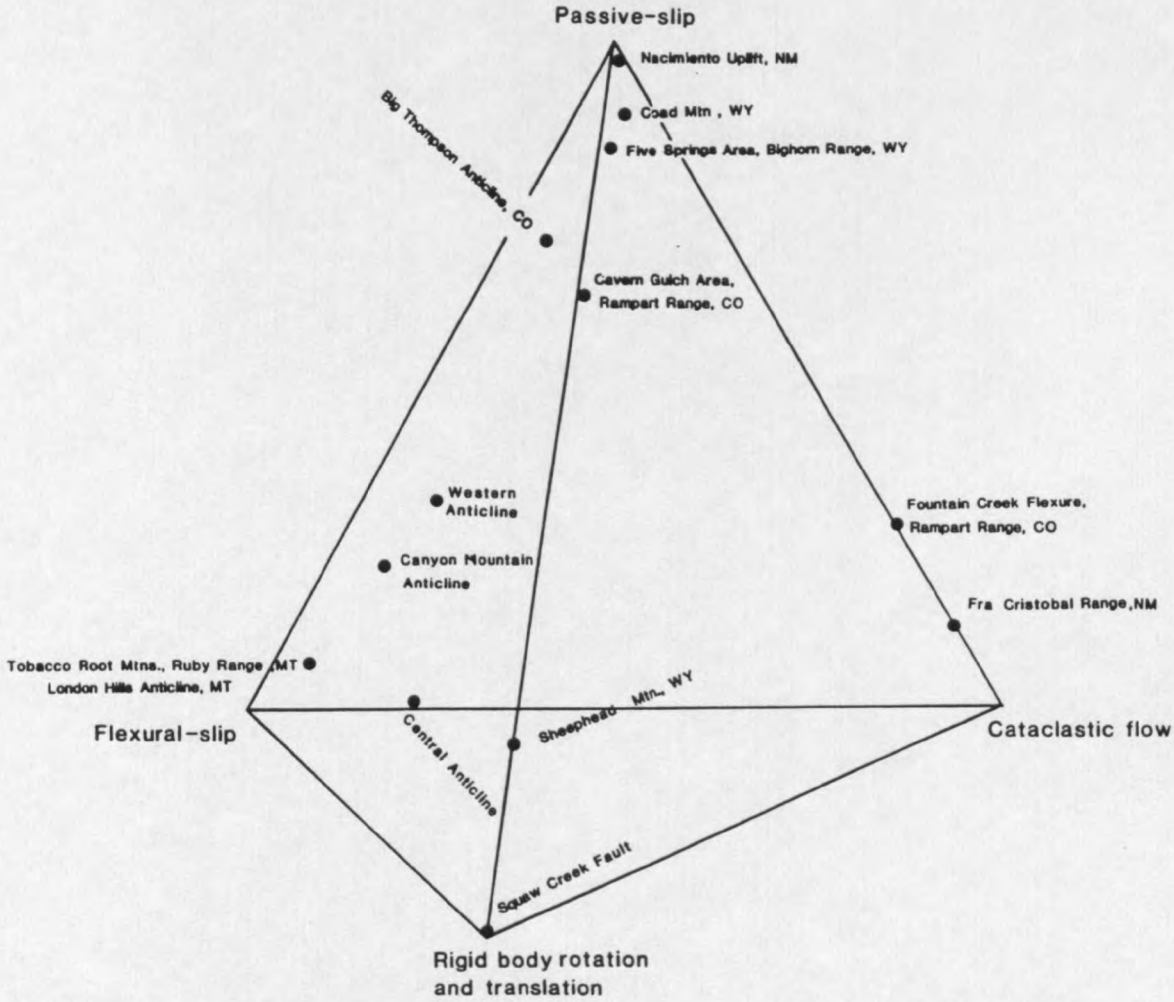

Figure 38. Detailed field investigations of basement deformation in the cores of Laramide folds show the basement was folded by cataclastic flow, passive-slip, and flexural-slip. A continuous transition exists between rigid body response and passive-slip which depends on the scale of observation. Sources and a description of each study is given in Table 1.

Passive-slip folding and cataclastic flow are limited to rocks where lithologic layering played no role in the deformation. This is indicated by the predominance of igneous rocks deforming by these mechanisms (Table 1) (Barnes and Houston, 1970; Chapin and Nelson, 1986; Hudson, 1955). The transition from passive-slip folding to cataclastic flow occurs with increased fold curvature. Evidence for this transition is provided by two studies of the Fountain Creek flexure in the Rampart Range of Colorado (Hudson, 1955; Blanton, 1975).

In a tightly folded region of Fountain Creek flexure, deformation occurred by intense crushing (Hudson, 1955). Where the sedimentary cover was characterized by open folds, basement deformation was accommodated by movement along fractures and minor faults (Hudson, 1955)(Table 1). The outcrop where Hudson (1955) made these observations has since been destroyed by highway construction. In a later investigation, Blanton (1975) described numerous low angle faults at a structurally deeper level that were exposed by the highway construction. In the Cavern Gulch area immediately north of the Fountain Creek flexure, Blanton (1975) also recognized that broad, regional folding occurred by displacements of fault-bounded basement blocks (Figure 38) (Table 1). Thus, a transition from passive-slip to cataclastic flow occurs with increased fold curvature.

The western anticline, Canyon Mountain anticline, and Big Thompson anticline in the Front Range of Colorado contain evidence of a combination of flexural-slip and passive-slip folding (LeMasurier, 1970). Big Thompson anticline deformed primarily by "small scale distributive displacement along preexisting fractures" with minor

Table 1. Basement response in the cores of Laramide folds based on detailed filed observations.

Location	Lithology	Response	Source
Fra Cristobal Range, NM	Granite	Cataclastic flow along closely spaced fractures	Chapin and Nelson (1986)
London Hills anticline, MT	Quartzofelds-pathic gneiss, amphibolite	Flexural-slip along compositional layering	Wagner (1957)
Tobacco Root Mtns., Ruby Range, MT	Quartzofelds-pathic gneiss, marble, schist	Flexural-slip along compositional layering	Schmidt and Garihan (1983)
Sheephead Mtn., WY	Quartzofelds-pathic gneiss	Rigid body, SE portion shows mobile response along closely spaced fractures	Banks (1969)
Coad Mtn., WY	Granitic augen gneiss	Passive-slip along axial planar fractures	Barnes and Houston (1970)
Five Springs Area, NW flank, Big Horn Range, WY	Biotite-quartz-oligioclase gneiss	Block tilting and rotation along closely spaced fractures with reverse displacement	Hoppin (1970)
Nacimiento Uplift, NM	Quartz monzonite	Passive slip folding by shear along closely spaced fractures	Woodward and others (1972)
Big Thompson Anticline, Front Range, CO	Mica schist, feldspathic quartzite, aplite, pegmatite	Small scale distributive displacement along pre-existing fractures with minor flexural-slip adjacent to bounding fault	LeMasurier (1970)
Fountain Creek Flexure, Rampart Range, CO	Granite	Intense crushing in tightly folded region, fracturing and and minor faulting where folds are open	Hudson (1955)
Cavern Gulch, Rampart Range, CO	Granite	Open regional folds occur by fault bounded blocks	Blanton (1975)

foliation parallel slip occurring adjacent to the bounding fault (LeMasurier, 1970). The western anticline, on the other hand, deformed primarily by flexural- slip; however, passive-slip was important in regions of Archean folding. Canyon Mountain anticline shows foliation-parallel faulting in the core indicating some shortening occurred by passive-slip, in addition to flexural-slip folding. Compositional layering played some role in deformation in each of these structures.

Big Thompson anticline, Colorado and Sheephead Mountain, Wyoming are commonly referenced as examples where the basement deformed as a rigid body (Matthews, 1986)(Table 1). The aforementioned mobile basement response at Big Thompson anticline is compatible with Berg's fold-thrust model (LeMasurier, 1970). However, eight kilometers to the south, in a structurally lower level of the fold, three large blocks, bounded by high angle reverse faults, accommodated deformation (Prucha and others, 1965). Sheephead Mountain is similar to the Big Thompson anticline in this respect. No significant rotations of Precambrian fabric were noted in the core of the fold or along the moderately (30^{o}) dipping west limb (Banks, 1969). However, along the overturned southeast limb, fractured basement gneiss is overlain by equally fractured Madison Limestone (Banks, 1969). Both examples of supposed rigid basement actually indicate a mobile basement response in the vicinity of the curved, basement nonconformity.

A rigid body response is shown as a deformational end member in Figure 38 with Squaw Creek fault as an example. The deformation at Cavern Gulch area (Blanton, 1975) occurred by rigid body movements and passive-slip. Squaw Creek fault and the Cavern Gulch area illustrate

that a continuum exists between rigid body deformation and passive-slip folding. The distinction is a matter of scale of observation (Woodward, 1986).

The mechanics of deformation in the transition zone between folded and unfolded basement remains a mystery. A transition from conical to cylindrical folding, shown in the western anticline (Figure 5), indicates that a zone exists close to the upper basement surface where deformation is independent of the overlying Paleozoic rocks and underlying basement. Apparently faulting and foliation-parallel shear disengages the lower basement from this zone. In the study area, well-developed foliation surfaces allowed the lower basement to fold, whereas, in the Big Thompson area the lower basement deformed by block faulting.

In conclusion, a test of the validity of the fold and non-fold models by examining field relations indicates that active basement folding of the upper basement surface accompanied compressive buckling of overlying sedimentary rocks (Berg, 1962). Folding of the basement occurred by a spectrum of mechanisms. A transition from passive-slip to cataclastic flow occurs with increased deformation in mechanically isotropic rocks. A transition from passive-slip to flexural-slip folding occurs with an increased number of fortuitously oriented foliation surfaces. The non-fold model (Erslev, 1986; Stone, 1984) is valid in regions shortened by faulting with no folding of the overlying sedimentary strata.

CONCLUSIONS

1. Laramide Basement Geometry - Canyon Mountain anticline and the anticlines of the Bridger Range have folded basement in their cores. A transition from conical folding to cylindrical folding occurs with increased distance from the upper basement surface in at least one anticline. Squaw Creek fault has a planar upper basement surface and an absence of rotated foliations.

2. Kinematics of Basement Deformation - The angle of discordance between the Cambrian Flathead Sandstone and basement foliation surfaces exerted a fundamental control over the basement response. In regions where the angle of discordance was high (Squaw Creek fault), the basement deformed by rigid body movements. Where the angle of discordance was low, folding of the basement occurred. Basement folding occurred primarily by oblique flexural-slip along preexisting foliation surfaces. Passive-slip was predominant in regions where Archean folding blocked foliation-parallel glide planes. Break up of the folded layer into large (5 - 12 m), internally undeformed blocks was preferred over coherent deformation with large amounts of tangential longitudinal strain.

3. Shear Zone Deformation - Shear zones were characterized by minimum temperature and pressure conditions of 200°C and 670 bars. Thick cataclastic shear zones bound macrogranular blocks where large amounts of shear strain were accommodated. Deformation in these zones occurred

by brittle and brittle-ductile processes. With decreased grain size and increased fluid influx, a transition from mechanical fracturing and frictional sliding to pressure solution glide occurred. Metamorphism was deformation-enhanced and occurred under saturated conditions.

4. Models of Foreland Uplifts - The folded basement of the southern Bridger Range and northeastern Gallatin Range is compatible with the fold-thrust model (Berg, 1962). Squaw Creek is most closely modeled by the thrust-fold model (Stone, 1984; Erslev, 1986), although there is no indication of force folding in the overlying strata. Comparisons with deformational mechanisms found in other basement-cored anticlines indicates the basement folds by a spectrum of mechanisms. Lithology, foliation orientation, and fold curvature are the predominant factors in determining whether flexural-slip, passive-slip, or cataclastic flow will predominate. Folded basement and an absence of major detachments and force folds strongly suggest that active basement folding accompanies folding of overlying Paleozoic strata.

REFERENCES CITED

Allmendinger, R.W., 1986, Tectonic development, southeastern border of the Puna Plateau, northwestern Argentine Andes: Geological Society of America Bulletin, v. 97, p. 1070 - 1082.

Banks, C.E., 1969, Precambrian gneiss at Sheephead Mountain, Carbon County, Wyoming, and its relation to Laramide structure: Contributions to Geology, University of Wyoming, R.B. Parker (ed.), v. 8, no. 1, p. 54-64.

Barnes, C.W., and Houston, R.S., 1970, Basement response to the Laramide orogeny at Coad Mountain, Wyoming: Contributions to Geology, University of Wyoming, R.B. Parker (ed.), v. 9, no. 2, p. 37-41.

Berg, R.R., 1962, Mountain flank thrusting in Rocky Mountain foreland, Wyoming and Colorado: American Association of Petroleum Geologists Bulletin, v. 46, p. 2019-2032.

Best, M.G., 1982, Igneous and Metamorphic Petrology: W.H. Freeman and Company, San Francisco, 630 p.

Blackstone, D.L., 1940, Structure of the Pryor Mountains, Montana: Journal of Geology, v. 48, p. 590-618.

_____, 1980, Foreland deformation - compression as a cause: Contributions to Geology, University of Wyoming, v. 18, p. 83 - 101.

Blanton, T.L., III, 1975, Fountain Creek flexure and basement deformation in the Manitou Spur: Mountain Geologist, v. 12, p. 119-126.

Brewer, J.A., Cook, F.A., Brown, L.D., Oliver, J.E., Kaufman, S., and Albaugh, D.S., 1981, COCORP seismic reflection profiling across thrust faults in Thrust and Nappe Tectonics: The Geological Society of London, p. 501-511.

Brewer, J.A., Smithson, S.B., Oliver, J.E., Kaufman, S., and Brown, L.D., 1980, The Laramide Orogeny: evidence from COCORP deep crustal seismic profiles in the Wind River Mountains, Wyoming: Tectonophysics, v. 62, p. 62, p. 165-189.

Brown, W.G., 1983, Sequential development of the fold-thrust model of foreland deformation in Lowell, J.D., (ed.), Conference on Rocky Mountain Foreland Basins and Uplifts: Rocky Mountain Association of Geologists Guidebook, p. 57-64.

Brown, W.G., 1984, A reverse fault interpretation of Rattlesnake Mountain anticline, Wyoming: Mountain Geologist, v. 21, p. 31-35.

Bruhn, R.L., and Beck, S.L., 1981, Mechanics of thrust faulting in crystalline basement, Sevier orogenic belt, Utah: Geology, v. 9, p. 200-204.

Chapin, M.A. and Nelson, E.P., 1986, Analysis of Laramide basement-involved deformation, Fra Cristobal Range, New Mexico: American Association of Petroleum Geologists, Annual Rocky Mountain Section meeting (abs.), Casper, Wyoming, in American Association of Petroleum Geologists Bulletin, v. 70, p. 1034.

Cook, D.G., 1983, The northern Franklin Mountains, Northwest Territories, Canada - a scale model of the Wyoming province, in Lowell, J.D., (ed.), Conference on Rocky Mountain Foreland Basins and Uplifts: Rocky Mountain Association of Geologists Guidebook, p. 315-338.

Craiglow, C.J., 1986, Tectonic significance of the Pass Fault, central Bridger Range, southwest Montana [M.S. thesis]: Bozeman, Montana, Montana State University, 40 p.

Donath, F.A., 1964, Strength variation and deformational behaviour in anisotropic rock in Judd, W.R., (ed.), State of Stress in the Earth's Crust: American Elsevier, New York, p. 281-297.

Donath, F.A., and Parker, R.B., 1964, Folds and Folding: Geological Society of America Bulletin, v. 75, p. 45-62.

Elliott, D., 1973, Diffusion flow laws in metamorphic rocks: Geological Society of America Bulletin, v. 84, p. 2645-2664.

_____, 1983, The construction of balanced cross sections: Journal of Structural Geology, v. 5, p. 101.

Engel, A.E.J., 1963, Geologic evolution of North America: Science, v. 140, p. 143-152.

Erhslev, E.A., 1985, Comment on balanced cross sections of small fold-thrust structures: Mountain Geologists, v. 22, p. 91-93.

_____, 1986, Basement blancing of Rocky Mountain foreland uplifts: Geology, v. 14, p. 259-262.

Gries, R., 1983, Oil and gas prospecting beneath Precambrian of foreland thrust plates in Rocky Mountains: American Association of Petroleum Geologists Bulletin, v. 67, p. 1-28.

Higgins, M.W., 1971, Cataclastic rocks: United States Geological Survey Professional Paper 687, 97 p.

Hobbs, E.B., Means, W.D., and Williams, P.F., 1976, An Outline of Structural Geology, John Wiley and Sons, Inc., New York, 571 p.

Hodgson, R.A., 1965, Genetic and geometric relations between structures in basement and overlying sedimentary rocks with examples from Colorado plateau and Wyoming: American Association of Petroleum Geologists Bulletin, v. 49, p. 935-949.

Hoppin, R.A., 1970, Structural development of Five Springs Creek Area, Bighorn Mountains, Wyoming: Geological Society of America Bulletin, v. 81, p. 2403-2416.

Hudson, F.S., 1955, Folding of unmetamorphosed strata superjacent to massive basement rocks: American Association of Petroleum Geologists Bulletin, v. 39, p. 2038-2052.

Hyndman, D.W., 1972, Petrology of Igneous and Metamorphic Rocks: McGraw-Hill Book Company, New York, 533 p.

James, H.L., and Hedge, C.E., 1980, Age of the basement of southwest Montana: Geological Society of America Bulletin, v. 91, no. 1, p. I 11-I 15.

Jordan, T.E., Isacks, B.L., Allmendinger, R.W., Brewer, J.A., Ramos, V.A., and Ando, C.J., 1983, Andean tectonics related to geometry of subducted Nazca plate: Geological Society of America Bulletin, v. 94, p. 341-361.

Lageson, D.R., and Miller, E.W., 1987, Finite strain and interaction of thrust belt and foreland deformation in the Bridger Range, Montana: in press.

_____ and Zim, J.C., 1985, Uplifted basement wedges in the northern Rocky Mountain foreland: Geological Society of America, Rocky Mountain Section, 38th Annual Meeting (abs.), Boise, Idaho., p. 250-251.

LeMasurier, W.E., 1970, Structural study of a Laramide fold involving shallow seated basement rock, Front Range, Colorado: Geological Society of America Bulletin, v. 81, p. 421-434.

Liou, J.G., 1973, Synthesis and stability relations of epiodote: Journal of Petrology, v. 14, pp.381-413.

Matthews, V. III, 1986, A case for brittle deformation of the basement during the Laramide revolution in the Rocky Mountain foreland province: The Mountain Geologist, v. 23, no. 1, p. 1-5.

May, K.A., 1985, Archean geology of a part of the northern Gallatin Range, southwest Montana [M.S. thesis]: Bozeman, Montana, Montana State University, 91 p.

McMannis, W.J., 1955, Geology of the Bridger Range, Montana: Bulletin of the Geological Society of America, v. 68, p. 1385-1430.

_____ and Chadwick, R.A., 1964, Geology of the Garnet Mountain quadrangle: Montana Bureau of Mines and Geology Bulletin, v. 43, 47 p.

Mitra, G., 1978, Ductile deformation zones and mylonites: the mechanical processes involved in the deformation of crystalline basement rocks: American Journal of Science, v. 278, p. 1057-1084.

_____ 1984, Brittle to ductile transition due to large strains along the White Rock thrust, Wind River Mountains, Wyoming: Journal of Structural Geology, v. 6, pp. 51-61.

Mitra, G. and Frost, R.B., 1981, Mechanisms of deformation within Laramide and Precambrain deformation zones in basement rocks of the Wind River Mountains: Contributions to Geology, University of Wyoming, v. 19, no. 2, p. 161-173.

Miyashiro, A., and Seki, Y., 1958, Enlargement of the composition field of epidote and piemontite with rising temperature: American Journal of Science, v. 256, p. 423-430.

Paterson, M.S., 1978, Experimental Rock Deformation - the brittle field: Springer - Verlag, 254 p.

Price, R.A., 1966, The tectonic significance of mesoscopic subfabrics in the southern Rocky Mountains of Alberta and British Columbia: Canadian Journal of Earth Sciences, v. 4, p. 39-70.

Prucha, J.J., Graham, J.A., and Nickelson, R.P., 1965, Basement controlled deformation in Wyoming Province of Rocky Mountain foreland: American Association of Petroleum Geologists Bulletin, v. 49, p. 966-992.

Ramsay, J.G., 1967, Folding and Fracturing of Rocks: McGraw-Hill Book Company, New York, 568 p.

_____, 1980, Shear zone geometry: a review: Journal of Structural Geology, v. 2, p. 83-99.

_____, and Huber, M.I., 1983, The Techniques of Modern Structural Geology, Volume 1: Strain Analysis: Academic Press, New York, 307 p.

Richards, P.W., 1957, Geology of the area east and southeast of Livingston, Park County, Montana: United States Geological Survey Bulletin 1021-1, 438 p.

Robbins, E.A., and Erslev, E.A., 1986, Basement wedges, back-thrusting and thin skinned deformation in the northwest Beartooth Mountains near Livingston, Montana in Yellowstone Bighorn Research Association Field Conference: Montana Geological Society, p. 111-123.

Roberts, A.E., 1972, Cretaceous and early Tertiary depositional and tectonic history of the Livingston area, southwestern Montana: United States Geological Survey Professional Paper 526-C, 119 p.

Ross, J.V., and McLynn, J.C., 1963, Concentric folding of cover and basement at Baselr Lake, N.W.T., Canada: Journal of Geology, v. 71, p. 644-652.

Schmidt, C.J., and Garihan, J.M., 1983, Laramide tectonic development in the Rocky Mountain foreland of southwestern Montana in Lowell, J.D., (ed.), Conference on Rocky Mountain Foreland Basins and Uplifts: Rocky Mountain Association of Geologists Guidebook, p. 271-294.

Seki, Y., 1972, Lower-grade stability limit of epidote in the light of natural occurrences: Journal of the Geological Society of Japan, v. 78, no. 8, p. 405-413.

Spang, J.H., Evans, J.P., and Berg, R.R., 1985, Balanced cross sections of small fold-thrust structures: The Mountain Geologist, v. 22, p. 41-46.

Stearns, D.W., 1971, Mechanisms of drape folding in the Wyoming Province: Wyoming Geological Association 23rd Annual Field Conference Guidebook, p. 125-143.

Stearns, D.W., 1978, Faulting and forced folding in the Rocky Mountain foreland, in Matthews, V. III, ed., Laramide folding associated with basement block faulting in the western United States: Geological Society America Memoir 151, p. 1-37.

Stone, D.S., 1984, The Rattlesnake Mountain, Wyoming debate: A review and critique of models: Mountain Geologist, v. 21, p. 36-46.

Turner, F.J., 1968, Metamorphic Petrology: McGraw-Hill Book Company, New York, 403 p.

Wagner, S.W., 1957, Effect of Laramide folding on previously folded Precambrian metamorphic rocks, Madison County, Montana [M.S. thesis]: Bloomingdale, Indiana, Indiana University, 26 p.

White, S., 1975, Tectonic deformation and recrystallization of oligioclase: Contributions to Mineralogy and Petrology, v. 50, p. 287-304.

Wilson, G., 1982, Introduction to Small Scale Structures: George Allen and Unwin, London, 128 p.

Wintsch, R.P., 1985, The possible effects of deformation on chemical processes in metamorphic fault zones: in Thompson, A.B., and Rubie, D.C., eds., Metamorphic Reactions, Kinetics Textures, and Deformation: Springer-Verlag, New York, 291 p.

Wojtal, S., and Mitra, G., 1986, Strain hardening and strain softening in fault zones from foreland thrusts: Geological Society of America Bulletin, v. 97, p. 674-687.

Woodward, L.A., 1986, A case for brittle deformation of the basement during the Laramide Revolution in the Rocky Mountain foreland province: discussion: The Mountain Geologist, v. 23, no. 3, p. 90-94.

Woodward, L.A., Kaufman, W.H., and Anderson, J.B., 1972, Nacimiento fault and related structures, northern New Mexico: Geological Society of America Bulletin, v. 83, p. 2383-2396.